Journal of Geography and Earth Sciences
June 2023, Vol. 11, No. 1, pp. 1-42
ISSN 2334-2447 (Print) 2334-2455 (Online)

Published by American Research Institute for Policy Development
DOI: 10.15640/jges.v11n1a1
URL: http://dx.doi.org/10.15640/jges.v11n1a1

Spatial and Temporal Analysis of Daily Measurements of $PM_{2.5}$ Air Pollution in Beijing, China

Tao Tang[1], Hutong Fan[2], Qiang Sun[3], Wenji Zhao[4]

Abstract:

Air particulate matter (PM2.5) pollution is a critical environment and human health problem. This research utilizes dailymeasurement data of PM2.5 air pollution of 27 air pollution monitoring stations during five-year period (2014-2018) to analyzethe spatial and temporal distribution patterns in Beijing, China. Five (5) sampling time periods daily were extracted from original hourly monitoring data during the study period, namely:morning peak traffic period (MPT); morning low traffic period (MLT); afternoon low traffic period (ALT); afternoon peak traffic period (APT); and midnight period (MIDN).

Mann-Kendall statistical test andPrincipal Component Analysis (PCA) were used to study temporal trend and variations. Geostatistical method of inverse distance weighted (IDW) interpolations was used to study the spatial distribution patterns. The results of Mann-Kendall Trend Analysis indicate $PM_{2.5}$ concentrations mainly show declining patterns of the four seasons during the five-year period with the p-values of summer, fall, and winter are smaller than 0.01. Some p-values during spring are between 0.01 to 0.05 indicatingweak decline trend.PCA analysis shows that the dailyPM2.5 concentrations reachthe highest in the winter season, and the lowest concentrations in the summer each year.The general trend during the five-year study period is declining. Results of spatial analysis indicate that north and northwest region encountered the lowest PM2.5 air pollutions. The highest PM2.5 air pollution occurred in the southern suburban areas.The results show that heat energy supply duringwinter season to buildings and houses is the greatest impact factor to PM2.5 air pollutions in Beijing.

[1] Department of Geosciences, Buffalo State University, State University of New York, 1300 Elmwood Ave., Buffalo, NY. 14222
[2] Supper-Map, Inc., No. A10, Jiuxianqiao North Road, Beijing, China
[3] Department of Mathematics, Buffalo State University, State University of New York, 1300 Elmwood Ave., Buffalo, NY. 14222
[4] Beijing Key Laboratory of Resources, Environment and GIS, College of Natural Resources, Environment and Tourist Management, Capital Normal University, No. 105, Northwest Third Ring Road, Beijing, China

Keywords: *PM2.5* air pollution, Spatial and temporal data analysis, heating supply impact on air pollution

1. Introduction

Air particulate matter (PM2.5) pollution is a critical environment and human health problem. The primary pollutant type of air pollution that causes lung cancer was ambient particulate matters equal or smaller than 2.5 micro-meters, PM2.5(Chen et al., 2014; Wu et al., 2021). The objective of this research is to analyze the officially published daily PM2.5 data from 2014 to 2018 by the Bureau of Environmental Protections, City of Beijing, China and find the temporal and spatial distribution patterns. The daily field measurements were conducted at the bureau's air pollution monitoring stations across the entire municipality. This research also analyzes the major sources and impacting factors of PM2.5 in the study area based on the spatial and temporal distribution patterns.

The original dataset covers a total of 35 field measuring stations with hourly measurements conducted daily for a total of five years from 2014 to 2018. Analyzing this big dataset of PM2.5 pollution can yield results with higher precision, accuracy, and consistency in comparison to the previous study (Tang et al., 2009; Tang et al., 2010). The first hypothesis of this research is that the PM2.5 pollution in Beijing was gradually reduced and mitigated chronologically during the study period with the introduction of "Air Pollution Prevention and Control Action Plan" in 2013. The "Air Pollution Prevention and Control Action Plan"is the most rigorous air pollution emission reduction policy enforced by the Chinese government during the last a few decades (Zhao et al., 2020). Secondly, the major concentrations of PM2.5 pollutant might come from different sources at different time periods. During the building heat supply time-period in the winter season each year, the major source of PM2.5 pollutant is from building heat supply facilities using coal or natural gas. During other seasons, the major contributions to the PM2.5 pollutant in Beijing is mainly from vehicle traffic emissions.

2. The Study Area and Data Acquisition

Beijing is located at the northern part of the North China Plain with 39.9042°N latitude and 116.4074°E longitude. The municipality is surrounded by the Yan Mountain from north, northwest, and west. The climate in Beijing can be characterized by relatively high precipitation and high temperature in the summer times; relatively dry and low temperature in the winter periods (Beck et al., 2020).Owing to the fast industrialization and urban expansion, Beijing has observed a sharp increase in the frequency of severe air pollution events since late 1980s. Since the year of 2012, Beijing municipal government committed the funding for its Bureau of Environmental Protections to select the sites and construct permanent stations of air pollution monitoring.

The Municipal Environmental Air Pollution Monitoring Center of the Beijing Bureau of Environmental Protections manages a total of 35 air pollution monitoring stations, which are in different districts or counties in both urban and suburb regions across the municipality. One of the examples of the air pollution monitoring sitesthat include the particle matter sampling is the Longevity West Palace sampling station in Beijing, which the $PM_{2.5}$ data wereused in this study (Figure 1).

Figure 1: The Air Pollution (including $PM_{2.5}$) Sampling Site and Equipment Setup in the Longevity West Palace

Hourly values of $PM_{2.5}$ air pollution were monitored and published by the Beijing Municipal Environmental Monitoring Center (http://www.bjmemc.com.cn/). The five-year period datasets of this research were downloaded by our research team at the Capital Normal University, Beijing, China. After the $PM_{2.5}$ source data was collected, we conducted manual examinations and evaluation of data quality. Eight (8) monitoring stations were removed owing to large quantity of "null" values in the database. We think that the instability of the data collecting computer caused this situation.Therefore, this research only used the datasets of remaining 27 air pollution monitoring stations located in both urban area and suburb area (Figure 2) across Beijing Municipality.

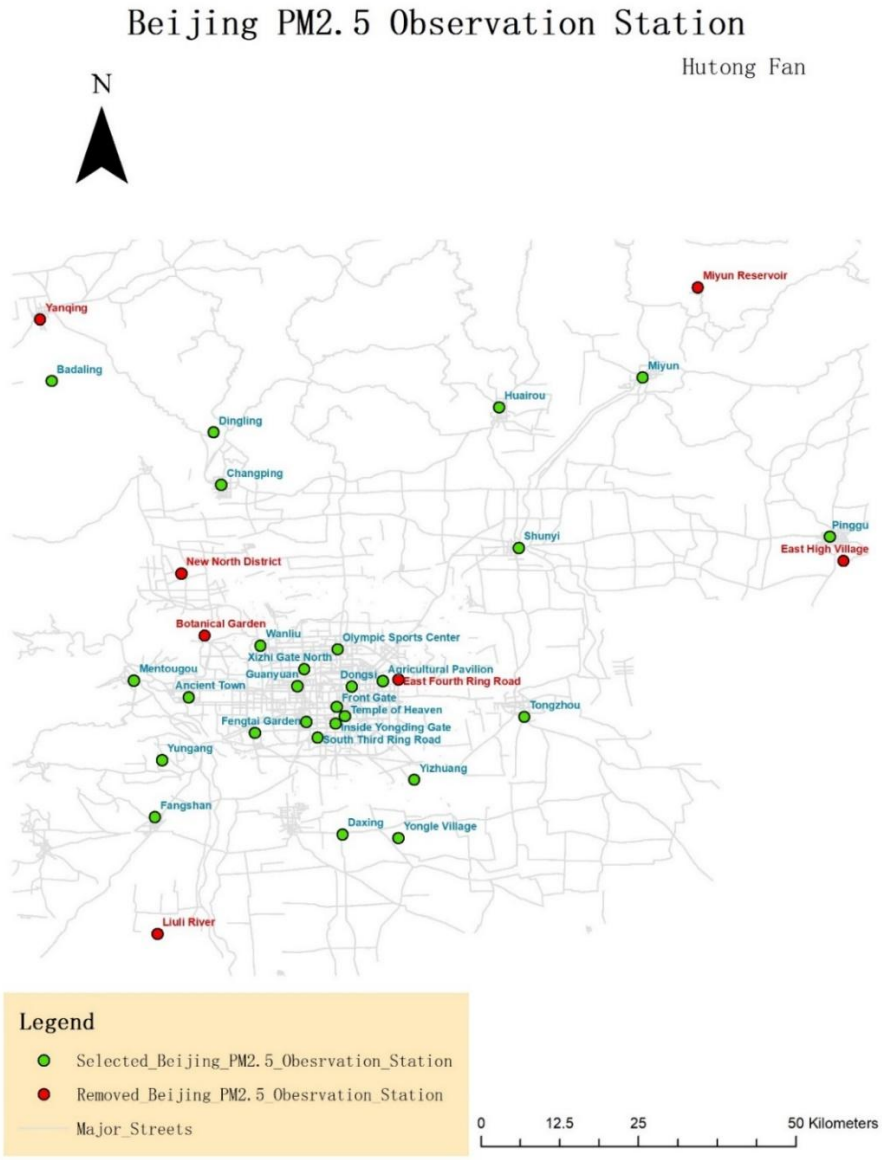

Figure 2: Map of Total $PM_{2.5}$ Observation Sites and the Sites Used in This Research in Beijing Municipality

3. Methods and Approaches

Fan et al. (2015) studied emission characteristics of vehicle exhaust based on actual traffic flow information in Beijing. The research analyzed the spatial and temporal distribution patterns of vehicle volume and pollutant emission quantities.

The research indicated there was a positive correlation between pollutant emission intensities and traffic volume. The emission intensity was generally higher during the daytime and high traffic hours than the evening hours. Based on the results of this research, we hypothesized the possible high and low pollution time periods during a 24-hour day. A total of five (5) sampling time periods within this large dataset were created for each of the monitoring days during the five-year period. These are: morning peak traffic time period (MPT, an average $PM_{2.5}$ concentration data from 06:00am and 08:00am); morning low traffic time period (MLT, an average $PM_{2.5}$ concentration data from 9:00am and 11:00am); afternoon low traffic time period (ALT, an average $PM_{2.5}$ concentration data from 01:00pm and 03:00pm); afternoon peak traffic time period (APT, an average $PM_{2.5}$ concentration data from 04:00pm and 06:00pm); and midnight time period (MIDN, an average $PM_{2.5}$ concentration data from 01:00am and 03:00am). MPT and APT are the commuting peak time in Beijing which have the maximum traffic flow on the streets and major highways. MLT and ALT are the sampling times during the working time periods of a day. Our objective is to find the contribution of human activities on the $PM_{2.5}$ pollutions in Beijing. To discover the potential contributions of $PM_{2.5}$ concentrations from heating supply to buildings and houses in Beijing, we also selected a mid-night sample period.

Data of sampling time periods were extracted using MATLAB software and stored in Excel. Python programming was applied to integrate those Excel charts into yearly differentiatedand air pollution monitoring site differentiated Excel sheets. A total of 135datasets were extracted for the 27 environmental air pollution observation sitesduring the entire five-year period. At each of 27 locations, we have five time periods that are namely: MIDN, MPT, MLT, ALT, and APT.

In order to capture the seasonal distribution and changes of the $PM_{2.5}$ air pollutions, one of the major approaches in this study is to divide the seasons in each year and calculate the mean values. Using a typical meteorological breakdown of seasons, we decided to use March, April, May in each year as months of spring season; June, July, August in each year as months of summer season; September, October, November in each year as months of autumn season; and December, January, February in each year as months of winter season. Then we calculated the seasonal average of $PM_{2.5}$ concentrations in each of the observation sites in each year and saved them into new datasets (Seasonal Average Selected Datasets). Seasonal Average Datasets of the selected five time periods during a data for each sampling year including all the observation stations were calculated.

3.1. Analyses of Temporal Distributions and Change of Air Pollutions in Beijing

In big data analysis, regression analysis is a predictive modeling technique that studies the relationship between a dependent variable (target) and the independent variables (predictors). This technique is often used for predictive analysis as well. In statistics, regression analysis refers to a statistical analysis method that determines the quantitative relationship between two or more variables that are depended on each other. We conducted basic analysis of simple seasonal or temporal pattern with the linear regression model of daily average $PM_{2.5}$ concentration data in R studio. Linear regression uses the best fitting line (regression line) to establish a relationship between the dependent variable (Y) and one or more independent variables (X).

In our study, daily variation or temporal change patterns were specified as the dependent variable and $PM_{2.5}$ concentrations as independent variable. The objective of this analysis is to present the general trend of slopes on decrease or increase of seasonal $PM_{2.5}$ concentrations with regression trend lines of linear regression model in the 5-year period. Simple regression trend lines can show the temporal patternsof general trends of seasonal variation on $PM_{2.5}$ pollutions in Beijing.

To show the significance of temporal trend in these sites, we conducted Mann-Kendall statistical test in the R studio. This method can effectively distinguish whether a natural process is in natural fluctuation or has a monotonic trend(Cao et al., 2008). Mann-Kendall nonparametric rank test is useful in trend detection of data. Its advantages are as follows, first, the series is allowed to have missing values. Secondly, it is no need to conduct specific distribution test for data series, and trend test can also be performed for extreme values. Thirdly, the analysis is mainly about the relative order of magnitude rather than the number itself, which enables the analysis of trace values or values below the detection range (Karmeshu, 2012).

Principal Component Analysis (PCA) is a multivariate statistical method to examine the correlation among multiple variables. PCA studies how to reveal the internal structure among multiple variables through a few principal components, deriving a few principal components from the original variables so that they retain as much information as possible about the original variables. The objective of using PCA in this research is to look for the major impact of pollution pattern among the five different sampling times during a day in five-year period in temporal scale for the entire five years.

We analyzed aggregative temporal patterns of the dataset with the principal component analysis (PCA) in MATLAB platform. The first step in PCA procedure is Data Arrangement. We converted the data from Excel worksheets into a MATLAB data file, which organized by location and year. In order to standardize the data, we subtracted the mean and divided by the standard deviation for values of each variable. The purpose of this step is to standardize the range of continuous initial variables so that each of them contributes equally to the analysis. The next step is the Covariance Matrix Computation. The purpose of this step is to understand how the variables in the input data set vary relative to each other's means, in order to determine the relationships between variables. Then, we computed the eigenvectors and eigenvalues of the covariance matrix to identify the principal components. The principal component with the highest variance is termed the "first principal component." To avoid protentional negative values in the process, which are meaninglessness in $PM_{2.5}$ concentration values, we only used the result of "first principal component". In the end, we recast the data along the axes of principal components. The purpose is to redirect the data from the original axes to the axes represented by the principal components using the eigenvectors formed by the eigenvectors of the covariance matrix.

The central idea of principal component analysis is to reduce the dimensionality of a data set composed of many related variables while preserving the variations existed in the data set as much as possible(Shlens, 2014). This objective is achieved by converting input variables to a new set of variables, known as principal components (PCS), which are unrelated and ordered so that the first few retains represent the most changes that occurred in all the original variables. The principal component represents the direction of the data that explains the largest amount of variance or changes over time.

That means the line that captures most of the information in the dataset. In this study, our objective is to find the principal component that represents the temporal variations of the entire time period during this 5-year on the hourly basis, which is a survey in this large database.

3.2. Analyses of Spatial Distributions of Air Pollutions in Beijing

Spatial interpolation is the process of estimating the values of the variables at unsampled locations with data of known observation points in the study region. Statistical interpolation methods were applied previously to air pollutant modeling to estimate the spatial distribution of air pollutions based on data provided by air quality monitoring sites (Lozano et al, 2009; Deligiorgiand Philippopoulos, 2011). There are two major categories of spatial interpolation techniquesin the Geographic Information Systems (GIS): deterministic and geostatistical. Proximity method, global polynomial (GPI), local polynomial (LPI), inverse distance weighted (IDW), and radial basis functions (RBF) interpolations are in general the deterministic methods. By contrast, geostatistical interpolation techniques includesurface trend and Kriging methods. Deterministic interpolation methods create prediction value surfaces with measured points based on degree of similarity and generatingsmoothness of value changes.Geostatistical methods quantify the spatial autocorrelation between measurement points and account the spatial configuration of sampling points around the predicted locations(Gimond, 2021).

The Inverse Distance Weighted (IDW) technique uses values from nearby weighted positions to calculate the average of unsampled positions. IDW interpolation explicitly assumes that things are close to one another are more alike than those that are further apart. It is expected that we will have more accurate result from IDW interpolation for those physically generated features or events. According to the research of Gimond (2021), the weight is proportional to the proximity of the sampling point to the unsampled position and can be specified by the IDW power coefficient. The bigger the power coefficient, the stronger the weight of nearby points as can be gleaned from the following equation that estimates the value $\hat{z}$ at an unsampled location *j:*

$$\hat{Z}_j = \frac{\sum_i Z_i / d_{ij}^n}{\sum_i 1 / d_{ij}^n}$$

The carat ^ above the variable $\hat{z}$ points out that the value at *j* is being estimated. The parameter *n* is the weight parameter that is applied as an exponent to the distance thus amplifying the irrelevance of a point at location *i* as distance to *j* increases.

IDW algorithm is actually a moving average interpolator that is typically applied to highly variable data. To predict a value for any unmeasured location, IDW uses the measured values surrounding the prediction location. In this study, we used the temporally sampled data that was calculated from observation stations to predict spatial distributions of $PM_{2.5}$ air pollutions. In addition, IDW assumes that the local effect of each of the measurement points decreases with increasing distance, which better reflects the geographic distribution pattern of the $PM_{2.5}$ in the city. In our study, we will make $PM_{2.5}$ concentration spatial interpolation maps for both annual average and seasonal average by five different sampling time periods for each of the 27 air pollution monitoring stations applying ArcGIS.

Standardization of digital maps of spatial interpolations on air particulate pollution was conducted for the purpose to compare analytical results. In this study, the legend in our annual average spatial interpolation atlas (Annual Average Atlas) of PM2.5 concentrations and seasonal average spatial interpolation atlas (Seasonal Average Atlas) for different daily sample time periods of PM2.5 concentrationswere standardized particularlyaccording to the real-world measured range of the entire survey time period.

For the annual average spatial interpolation atlas of $PM_{2.5}$ concentrations, we selected 5 ug/m^{3}as the legend group unit. All the maps in the annual average spatial interpolation atlas of $PM_{2.5}$ concentrations began at 50 ~ 55 ug/m^3 group and end at 95 ~ 100 ug/m^3 group. There are a 10 concentration groups in total. For the spatial interpolations atlas of seasonal average of $PM_{2.5}$ concentrations at different daily sample time periods, we found 27 ug/m^3 is the lowest $PM_{2.5}$ concentration, which is from APT time in the summer of 2018. The highest $PM_{2.5}$ concentration is 200 ug/m^3 and is from MIDN time in the winter of 2015. To guarantee the distinguishability of each map, we defined 18 concentration groups in total. For the Seasonal Average Atlas, we selected 10 ug/m^3 as the legend group unit. All the maps of seasonal spatial interpolation atlas of $PM_{2.5}$ concentrations in the different daily sample time periods began at 20 ~ 30 ug/m^3 group and end at 190 ~ 200 ug/m^3 group.

4. Results and Discussions

4.1 Results of Temporal Analysis of PM2.5 Air Pollution

Mann-Kendall Trend Analysis was conducted in the R studio. p-values were used as the major criterium to determine if a decrease or increase trend exist during the study period in different seasons. The null hypothesis is that there is no obvious up or down trend within the five-year period for different seasons. The statistical conditions were tested as the following. If p-value < 0.01, the description of the result is a stronger determination in rejecting the null hypothesis. If p-value is between 0.01 and 0.05, the description of the result is a weaker determination in rejecting the null hypothesis. If p-value > 0.05, it indicates that the results are more inclined to accept the null hypothesis.

Table 1 summarizes the result of slope and p-value of spring season trend lines at different monitoring stations during the five-year period. Examples of the trend line plots are shown in Figure 3. Table 1 is sorted by the slope rate from lowest to highest. We can find p-values of several sites are between 0.01 and 0.05 (green section) or higher than 0.05 (orange section)in Table 1. 11 of 27 $PM_{2.5}$ observation sites indicate that there are significant descending trends of $PM_{2.5}$ contaminant concentrations in the spring season during the five-year period. Another 11 of 27 $PM_{2.5}$ observation sites show there are weak descending trends of $PM_{2.5}$ contaminant concentrations in the spring season during the entire five-year period. 5 out of 27 $PM_{2.5}$ observation sites show that no obvious up or down trends of $PM_{2.5}$ contaminant concentration exist in the spring season during the five-year period.We can clearly identify the differences of the slope of trend linesin Figure 3. Although the variance of p-value results exists, majority of $PM_{2.5}$ observations (22 of 27) show descending trend (significant or weak trend) during the spring season of five years. Comparing different locations of the $PM_{2.5}$ observation sites in the spring (Table 1), all the five (5)sampling sites with no obvious variation trends are located in the suburban areas in Beijing.

Station-Name	Spring Slope	P-value
Fangshan	-0.0842	<0.01
South Third Ring Road	-0.07639	<0.01
Yungang	-0.07217	<0.01
Yizhuang	-0.07102	<0.01
Daxing	-0.0642	<0.01
Fengtai Garden	-0.06266	<0.01
Inside Yongding Gate	-0.06159	<0.01
Agricultural Pavilion	-0.05878	<0.01
Tongzhou	-0.05798	<0.01
Wanliu	-0.05735	<0.01
Olympic Sports Center	-0.05692	<0.01
Front Gate	-0.05393	0.01019
Temple of Heaven	-0.05079	0.01083
Shunyi	-0.04966	0.02043
Yongle Village	-0.04934	0.01412
Huairou	-0.04844	0.01377
Longevity West Palace	-0.04674	0.02326
Pinggu	-0.04505	0.02396
Guanyuan	-0.0436	0.03119
Dongsi	-0.04342	0.04226
Changping	-0.04183	0.03521
Xizhi Gate North	-0.04166	0.04641
Ancient Town	-0.04018	>0.05
Dingling	-0.03518	>0.05
Mentougou	-0.03273	>0.05
Miyun	-0.01769	>0.05
Badaling	0.000885	>0.05

Table 1: Results of Slope rate and P-value from Five-year Spring Sampling Trend Line

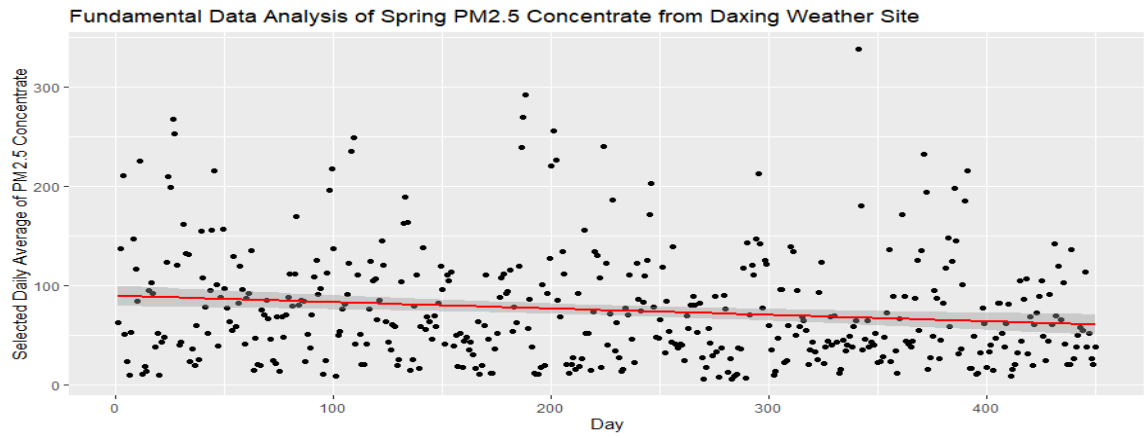

a)

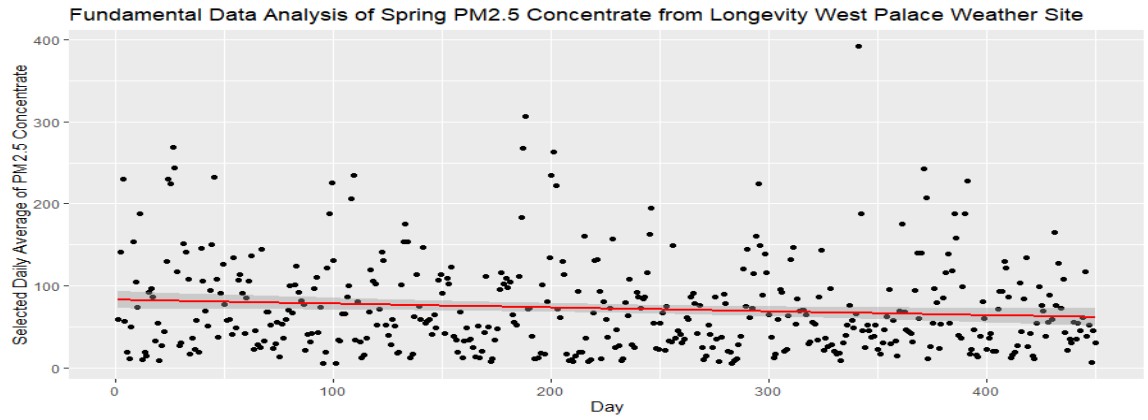

b)

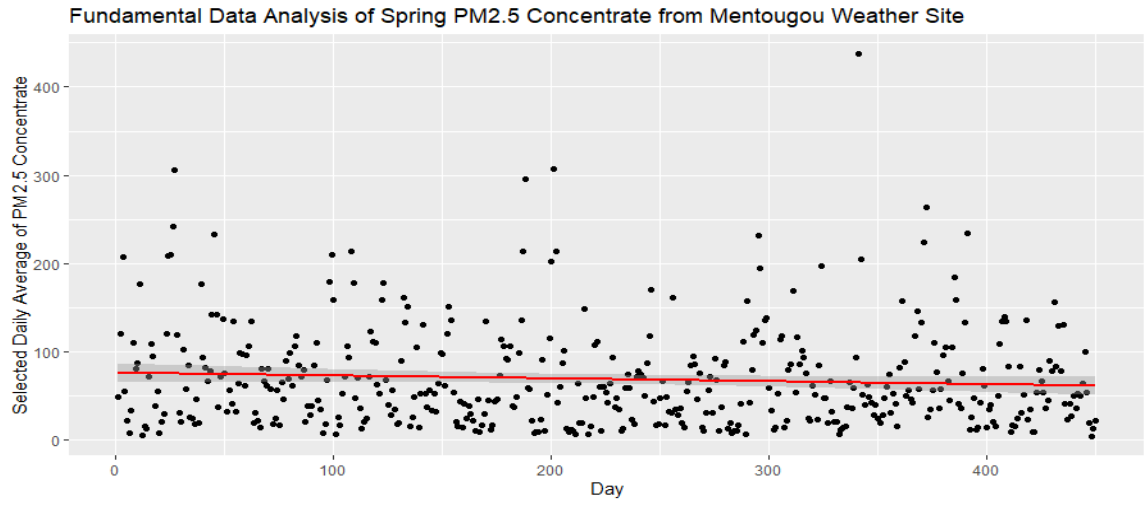

c)

Figure 3: Examples of Different Trend Conclusions in Spring
a) Daxing ($p < 0.01$), b) Longevity West Palace ($0.01 < p < 0.05$), c) Mentougou ($p > 0.05$)

Table 2 presents the result of slopes and p-values of trend lines for the summer during the five-year period, sorted by slope rate from lowest to highest. All the p-values of $PM_{2.5}$sampling sites are less than 0.01. Comparing with negative slope rates, all the $PM_{2.5}$ observation stations show there are significant decreasing trends of $PM_{2.5}$ contaminant concentration during the summer of five-year period.

Station-Name	Summer Slope	P-value
South Third Ring Road	-0.11223	<0.01
Yizhuang	-0.1022	<0.01
Daxing	-0.1004	<0.01
Guanyuan	-0.08778	<0.01
Tongzhou	-0.08653	<0.01
Olympic Sports Center	-0.08599	<0.01
Temple of Heaven	-0.08449	<0.01
Dongsi	-0.08321	<0.01
Front Gate	-0.08149	<0.01
Yungang	-0.08036	<0.01
Shunyi	-0.07902	<0.01
Pinggu	-0.07718	<0.01
Fangshan	-0.07604	<0.01
Wanliu	-0.07571	<0.01
Huairou	-0.07538	<0.01
Inside Yongding Gate	-0.07533	<0.01
Fengtai Garden	-0.07304	<0.01
Yongle Village	-0.07204	<0.01
Longevity West Palace	-0.06851	<0.01
Ancient Town	-0.06802	<0.01
Agricultural Pavilion	-0.06619	<0.01
Changping	-0.06546	<0.01
Dingling	-0.05571	<0.01
Mentougou	-0.04885	<0.01
Xizhi Gate North	-0.04631	<0.01
Badaling	-0.04514	<0.01
Miyun	-0.04451	<0.01

Table 2: Results of Slope rate and P-value from Five-year Summer Sampling Trend Line

Table 3 shows the result of slopes and p-values of autumn season during the five-year period, sorted by slope rate from lowest to highest. All the p-values of $PM_{2.5}$ observation sites are less than 0.01. Comping with negative slope rates, all the $PM_{2.5}$ observation sites show the trends of significant decrease of $PM_{2.5}$ contaminant concentration during the autumn of five-year period.

Station-Name	Autumn Slope	P-value
Yizhuang	-0.1553	<0.01
Daxing	-0.14174	<0.01
Front Gate	-0.12925	<0.01
South Third Ring Road	-0.12858	<0.01
Inside Yongding Gate	-0.12808	<0.01
Agricultural Pavilion	-0.12265	<0.01
Xizhi Gate North	-0.12028	<0.01
Fangshan	-0.11945	<0.01
Fengtai Garden	-0.11504	<0.01
Tongzhou	-0.11134	<0.01
Wanliu	-0.10973	<0.01
Yungang	-0.1071	<0.01
Yongle Village	-0.10435	<0.01
Olympic Sports Center	-0.1021	<0.01
Longevity West Palace	-0.09932	<0.01
Temple of Heaven	-0.09929	<0.01
Guanyuan	-0.09921	<0.01
Ancient Town	-0.09762	<0.01
Dingling	-0.09262	<0.01
Changping	-0.0917	<0.01
Dongsi	-0.08727	<0.01
Shunyi	-0.0828	<0.01
Huairou	-0.0809	<0.01
Mentougou	-0.07568	<0.01
Pinggu	-0.07493	<0.01
Miyun	-0.07254	<0.01
Badaling	-0.06505	<0.01

Table 3: Results of Slope rate and P-value from Five-year Autumn Sampling Trend Line

Table 4 indicates the result of slopes and p-values for winter during the five-year period, sorted by slope rate from lowest to highest. All the p-values of $PM_{2.5}$ observation sites are less than 0.01. Comparing the negative slope rates, all the $PM_{2.5}$ observation sites show there are significant decreasing trends of $PM_{2.5}$ contaminant concentrations in winter of the five-year period.

Station-Name	Winter Slope	P-value
Daxing	-0.24024	<0.01
Fangshan	-0.22595	<0.01
Tongzhou	-0.22527	<0.01
Yizhuang	-0.221	<0.01
Yongle Village	-0.20937	<0.01
Fengtai Garden	-0.19942	<0.01

South Third Ring Road	-0.19311	<0.01
Yungang	-0.18349	<0.01
Olympic Sports Center	-0.1822	<0.01
Front Gate	-0.17994	<0.01
Longevity West Palace	-0.17907	<0.01
Wanliu	-0.17718	<0.01
Agricultural Pavilion	-0.17653	<0.01
Inside Yongding Gate	-0.16561	<0.01
Pinggu	-0.165	<0.01
Dongsi	-0.15862	<0.01
Changping	-0.15601	<0.01
Ancient Town	-0.1541	<0.01
Guanyuan	-0.15385	<0.01
Temple of Heaven	-0.15187	<0.01
Huairou	-0.15095	<0.01
Dingling	-0.15053	<0.01
Xizhi Gate North	-0.14904	<0.01
Shunyi	-0.1459	<0.01
Miyun	-0.13578	<0.01
Mentougou	-0.13316	<0.01
Badaling	-0.09116	<0.01

Table 4: Results of Slope rate and P-value from Five-year Winter Sampling Trend Line

According to the p-values of four tables during four seasons, $PM_{2.5}$ concentrations mainly show declining patterns during the five-year period. Figure 4 is the computational results of Mann-Kendall Trend lines of different seasons during the five-year period at the Daxing samplingstationas an example. The slope rates at Daxing sampling site are -0.0642, -0.1004, -0.14174, -0.24024 in spring, summer, fall, and winter.

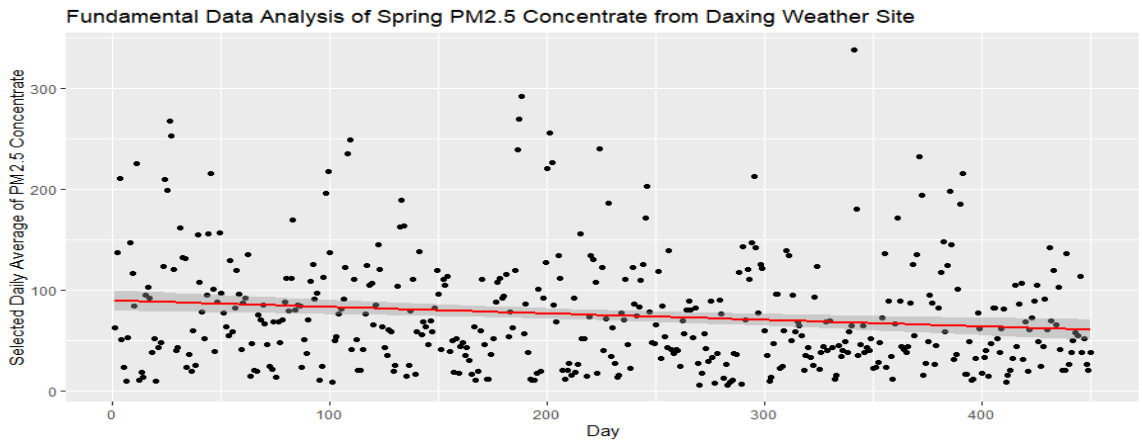

a)

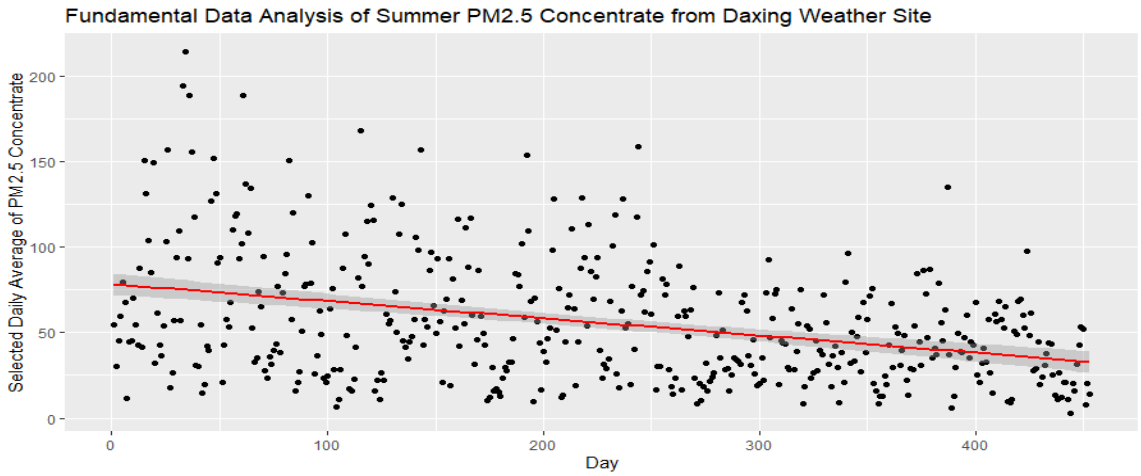

b)

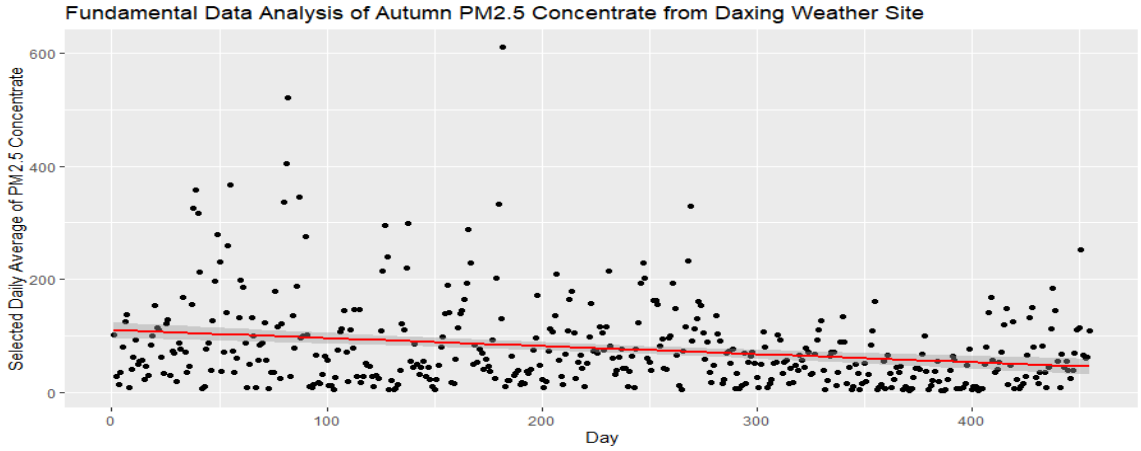

c)

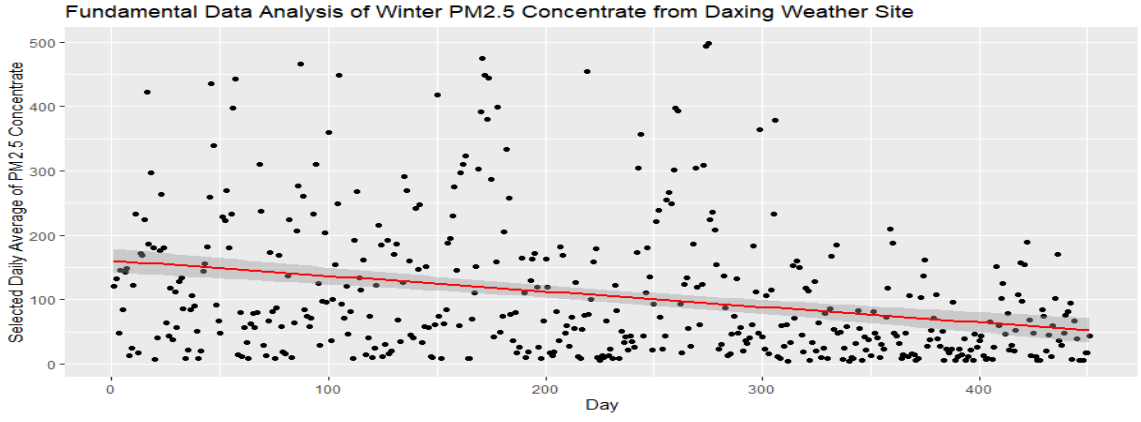

d)

Figure 4: Example: Five-year Different Seasons of $PM_{2.5}$ Contaminant Result
a) Spring, b) Summer, c) Autumn, d) Winter in Daxing Station

Principal component analysis (PCA) was conducted in the MATLAB environment. All the plots with five eigenvalues and corresponding weight percentage were produced. To avoid protentional negative values in the computation process, which might be meaningless in $PM_{2.5}$ concentration value representations, we only used the result of "first principal component". There are a total of five eigenvalues in the computations. The result of this process shows that the lowest weight percentage of the fifth eigenvalues is 77.62% and the highest weight percentage of the fifth eigenvalues is 82.50% among the 27 field sampling stations. All of the weight percentage of the fifth eigenvalues are around 80%. These analytical results suggest that the fifth eigenvalues of all the sampling stations are the "first principal component" in our research period.

All of the PCA distribution plots ofthe 27 sampling stations for the "first principal component" were produced. Figure 5 shows examples of the PCA computations. It is important to point out that the unit on these diagrams are the unit of the $PM_{2.5}$pollution concentration Datasets (ug/m3). Examples of PCA of $PM_{2.5}$pollution sampling sites in Figure 5, representing urban and suburban areasin Beijingpresented the similar trend patterns with Figure 3 and Figure 4. Sites of Inside Yongding Gate and Xizhi Gate North are examples in the urban area in Beijing. Badaling site is an example in the north suburb in Beijing and Yongle Village site is located in the southern suburb in Beijing.

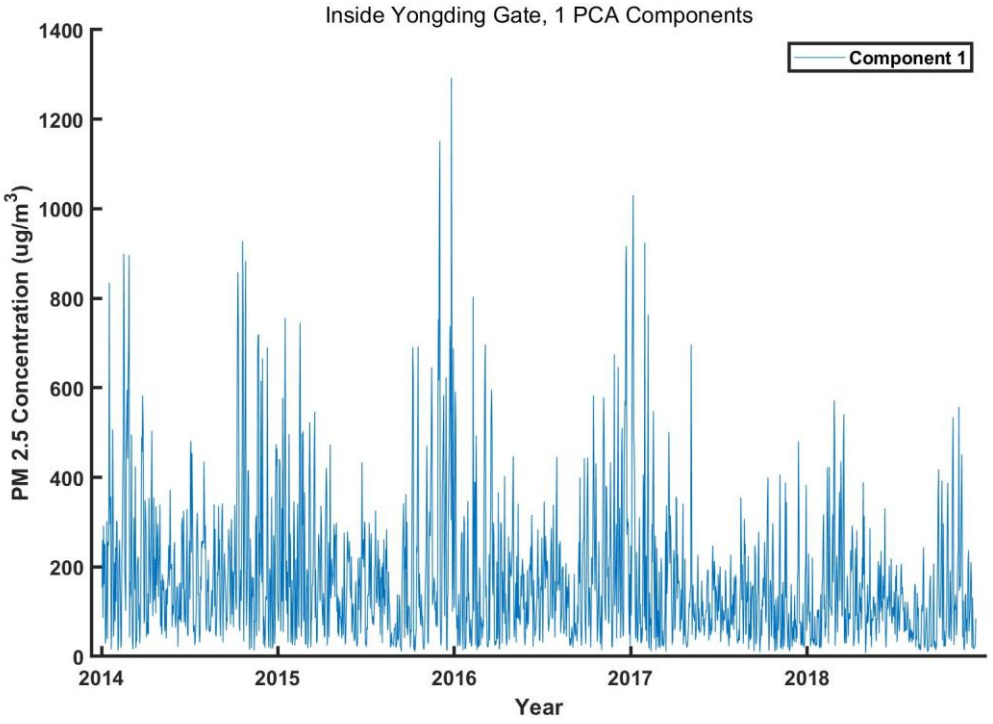

a)

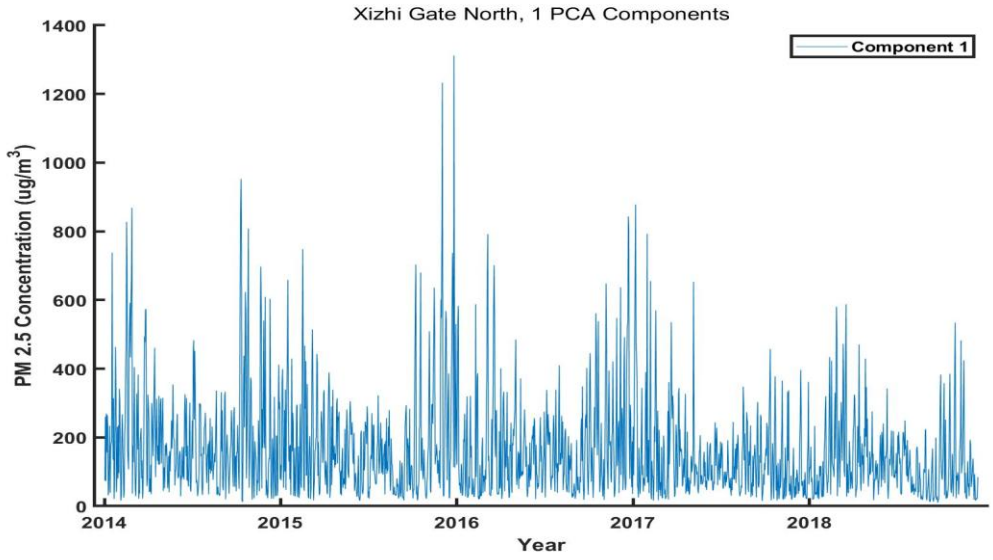
Xizhi Gate North, 1 PCA Components
Component 1
PM 2.5 Concentration (ug/m3)
1400
1200
1000
800
600
400
200
0
2014
2015
2016
2017
2018
Year

b)

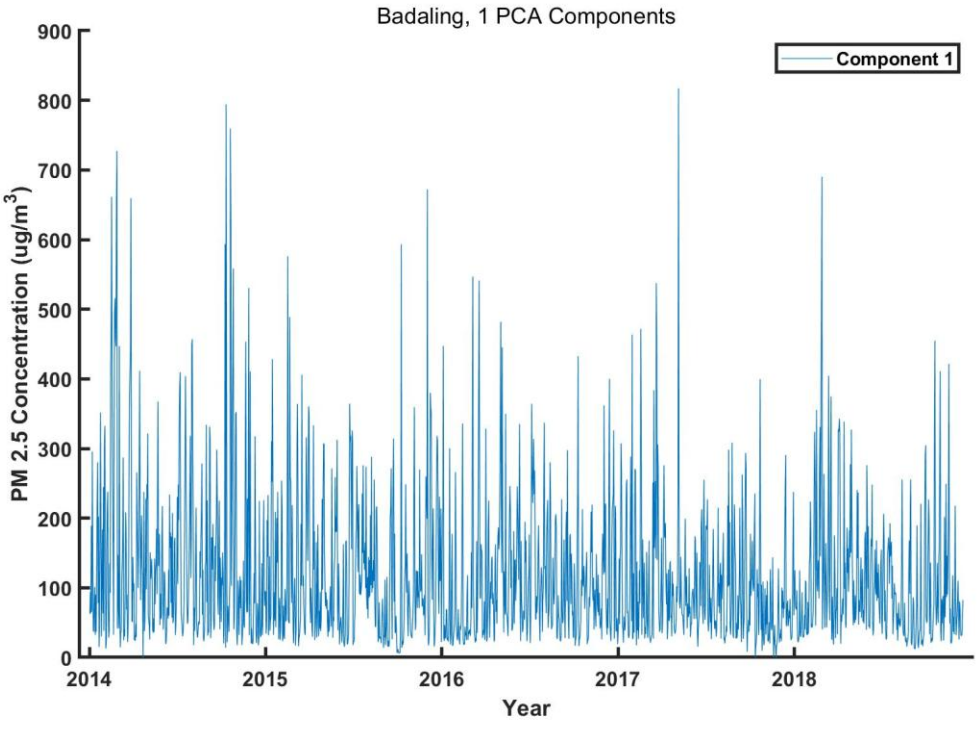
Badaling, 1 PCA Components
Component 1
PM 2.5 Concentration (ug/m3)
900
800
700
600
500
400
300
200
100
0
2014
2015
2016
2017
2018
Year

c)

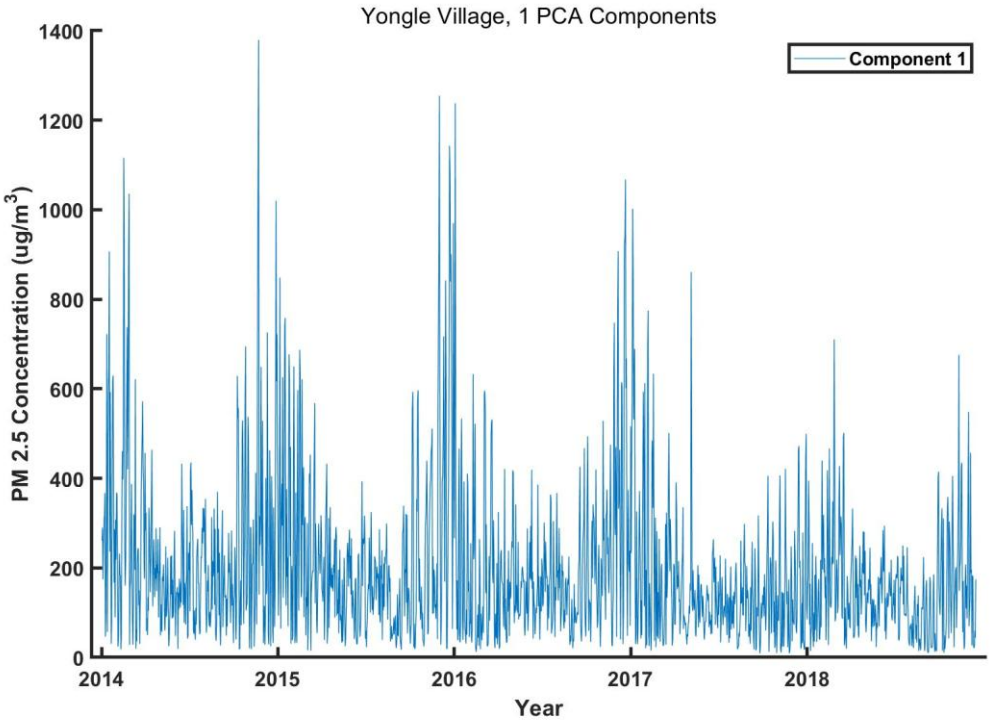

d)

Figure 5: PCA Results of Selected $PM_{2.5}$ Contaminant Observation Sites
a) Inside Yongding Gate, b) Xizhi Gate North, c) Badaling, d) Yongle Village

According to principles of the PCA analysis, PCA is designed for identifying the most significant aspects or characteristics of the dataset. In order to identify the significant temporal distribution patterns of large dataset, the PCA analysis replaces the original data with the most significant aspects of the data during the study time period. Therefore, PCA analysis is a suitable method to combine temporal variations in the five resampled time periods of $PM_{2.5}$concentrations using one single change curve of time series. The results of PCA time series pattern reflect the daily variations of $PM_{2.5}$concentrationsfor the entire 5-year period (Figure 5).

According to the resultsof PCA analysis, the general trends of $PM_{2.5}$ concentrations in Beijing at all 27 field sampling stations during the five-year study period show downwardstrend with daily and seasonal fluctuations. The $PM_{2.5}$ air pollution concentration values are relatively higher in the winter season each year. The $PM_{2.5}$ concentration time series pattern shows the values in winter reached the highest volumes each year while the year-to-year trend is decreasing. The $PM_{2.5}$ concentration time series pattern of PCA analysis also indicates the daily values reach the lowest in the middle of each year, normally during the late spring and summer. In summary, the results of this research suggest that the $PM_{2.5}$ concentrations are relatively low in summer and relatively high in winter in Beijing during the study period.

Each of the time series result plotsin this research showsthe $PM_{2.5}$ concentrations and pollution magnitudes day by day during the five-year study period. This is essential and significant for pinpointing when and where the most severe pollution situation occurred during the five-year period. Relating this daily pollution concentration time series to the respiratory disease treatment records that was collected by field hospital in the region, we will be able to analyze the potential causes. In the urban area in Beijing (Figure 5 a. and b.), the highest daily$PM_{2.5}$ concentration is around 1300 ug/m3. In the northern suburb of Beijing (Figure 5 c.) the highest daily $PM_{2.5}$ concentration is around 800 ug/m3. In the southern suburb of Beijing (Figure 9 d)) the highest daily $PM_{2.}$ concentration is around 1300 ug/m3. The $PM_{2.5}$ concentrations in the south suburban region is at the same level of magnitude to that of urban areas in Beijing. This result suggests that downtownBeijing is not the only high riskregion of $PM_{2.5}$ pollution. Secondly, this result also suggests that major sources of $PM_{2.5}$ air pollution might have been originated at southern part of the urban areas and southern suburban regions.

4.2 Results of Spatial Distribution Analysis of PM2.5 Air Pollution

Spatial distribution patterns of the average annual PM2.5 concentrations during the study period from 2014 to 2018 are shown in Figure 6. The legend of the entire five maps was standardized and the color presentations of the $PM_{2.5}$ air pollutions can be compared to each other. Pollution distribution patterns were interpolated using IDW (Inverse Distance Weighted) method in GIS. During this five-year study period, the highest annual average $PM_{2.5}$ concentration value ranges from95 to 100 ug/m3, and the lowest annual average $PM_{2.5}$ concentration value ranges from 50 to 55 ug/m3. The results show that the area encountering the highestannual $PM_{2.5}$ air pollutions is the south and southeast part of Beijing municipality. The area with the lowest $PM_{2.5}$ air pollutions is in the north and northwest region in Beijing. The results indicate that the highest $PM_{2.5}$ air pollution concentrations occurred in the southern suburban areas other than the downtown or core urban area in Beijing. This suggests that the southern suburban and urbanareas in Beijing arethe most polluted areas by $PM_{2.5}$. During the five-year study period, the annual $PM_{2.5}$ concentrations in Beijing aregradually reduced and air quality was improved.

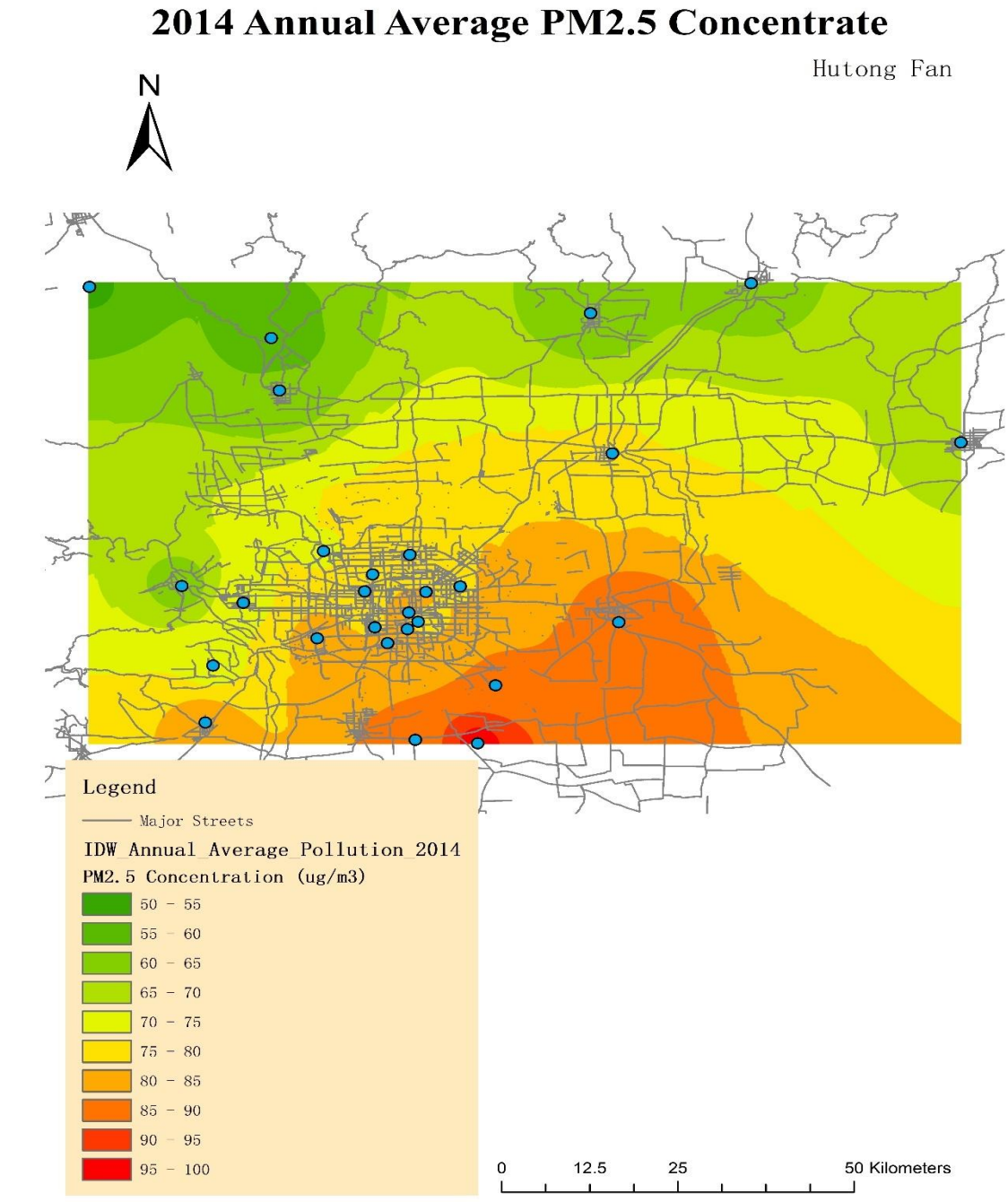
2014 Annual Average PM2.5 Concentrate
Hutong Fan
N
Legend
Major Streets
IDW_Annual_Average_Pollution_2014
PM2.5 Concentration (ug/m3)
50 - 55
55 - 60
60 - 65
65 - 70
70 - 75
75 - 80
80 - 85
85 - 90
90 - 95
95 - 100
0
12.5
25
50 Kilometers

a)

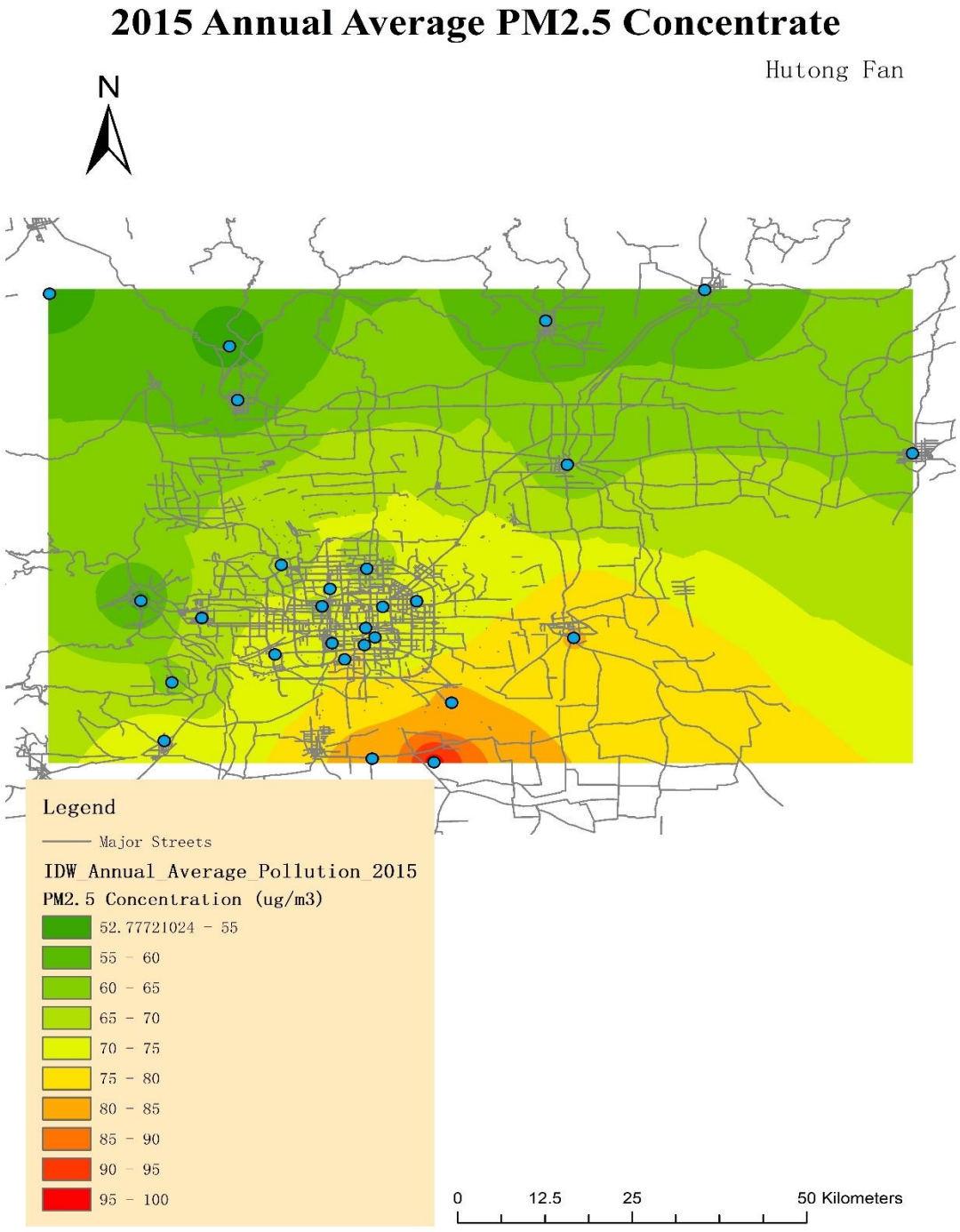
2015 Annual Average PM2.5 Concentrate
Hutong Fan
N
Legend
Major Streets
IDW_Annual_Average_Pollution_2015
PM2.5 Concentration (ug/m3)
52.77721024 - 55
55 - 60
60 - 65
65 - 70
70 - 75
75 - 80
80 - 85
85 - 90
90 - 95
95 - 100
0
12.5
25
50 Kilometers

b)

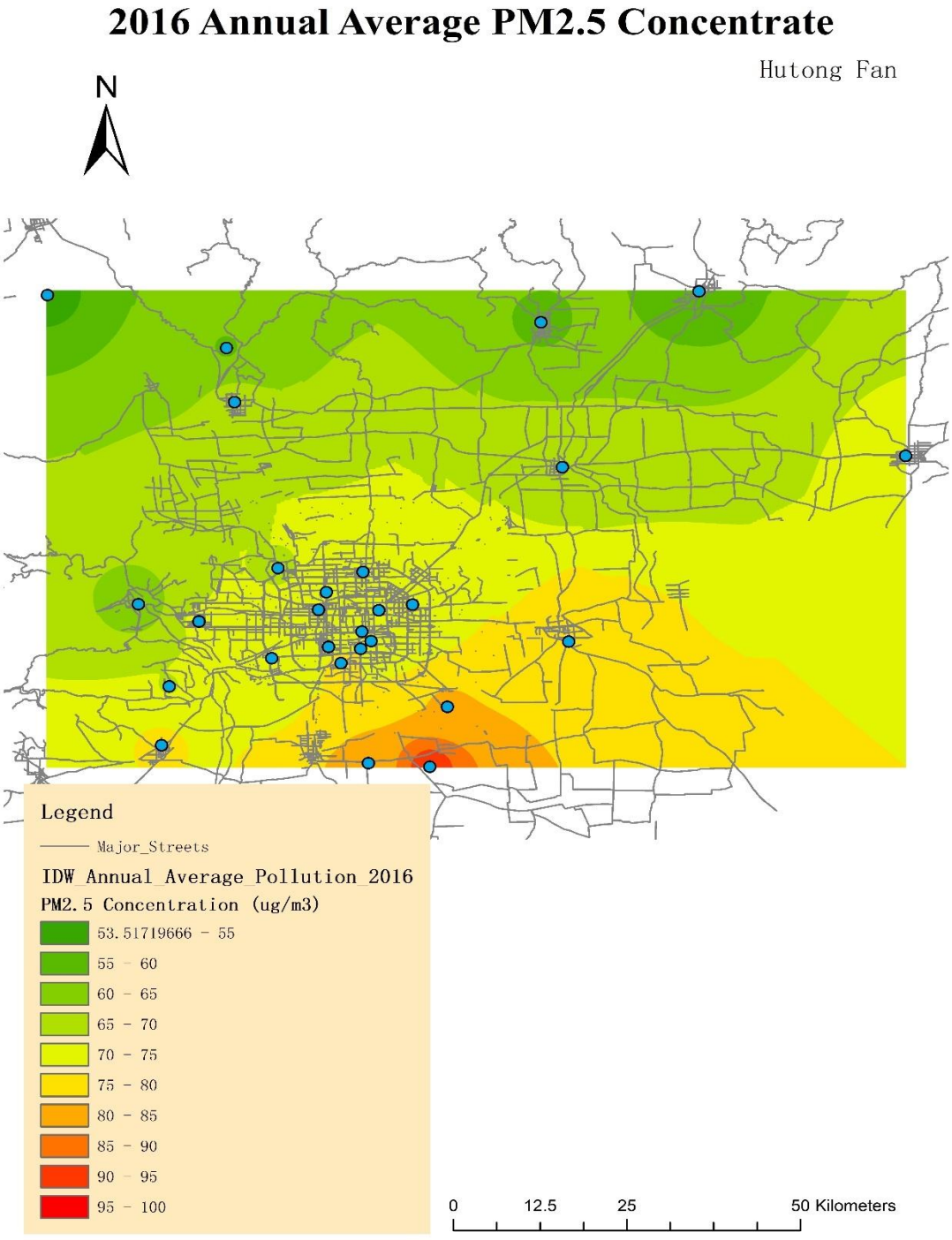
2016 Annual Average PM2.5 Concentrate
Hutong Fan
N
Legend
Major_Streets
IDW_Annual_Average_Pollution_2016
PM2.5 Concentration (ug/m3)
53.51719666 - 55
55 - 60
60 - 65
65 - 70
70 - 75
75 - 80
80 - 85
85 - 90
90 - 95
95 - 100
0
12.5
25
50 Kilometers

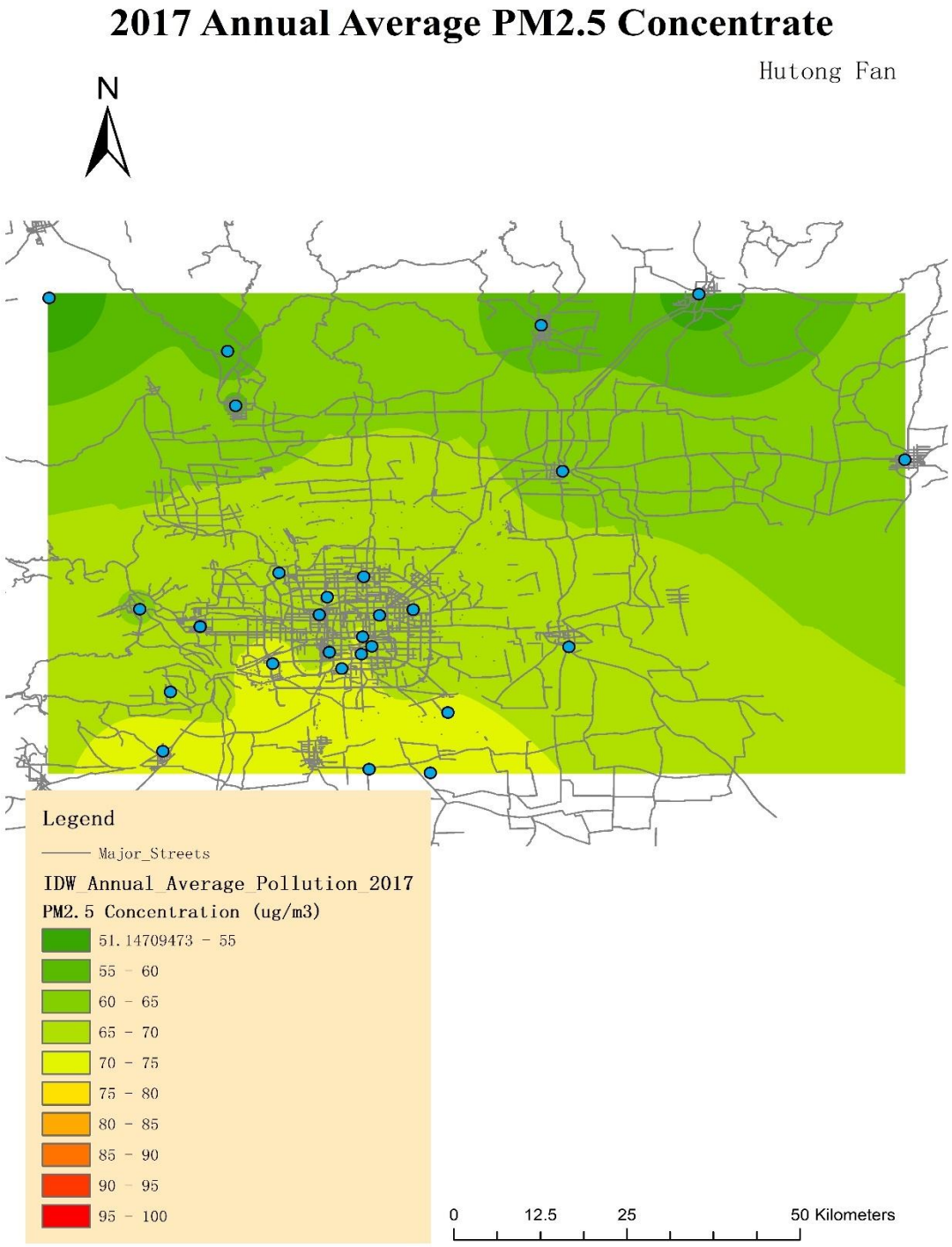
2017 Annual Average PM2.5 Concentrate
Hutong Fan
N
Legend
Major_Streets
IDW Annual Average Pollution 2017
PM2.5 Concentration (ug/m3)
51.14709473 - 55
55 - 60
60 - 65
65 - 70
70 - 75
75 - 80
80 - 85
85 - 90
90 - 95
95 - 100
0
12.5
25
50 Kilometers

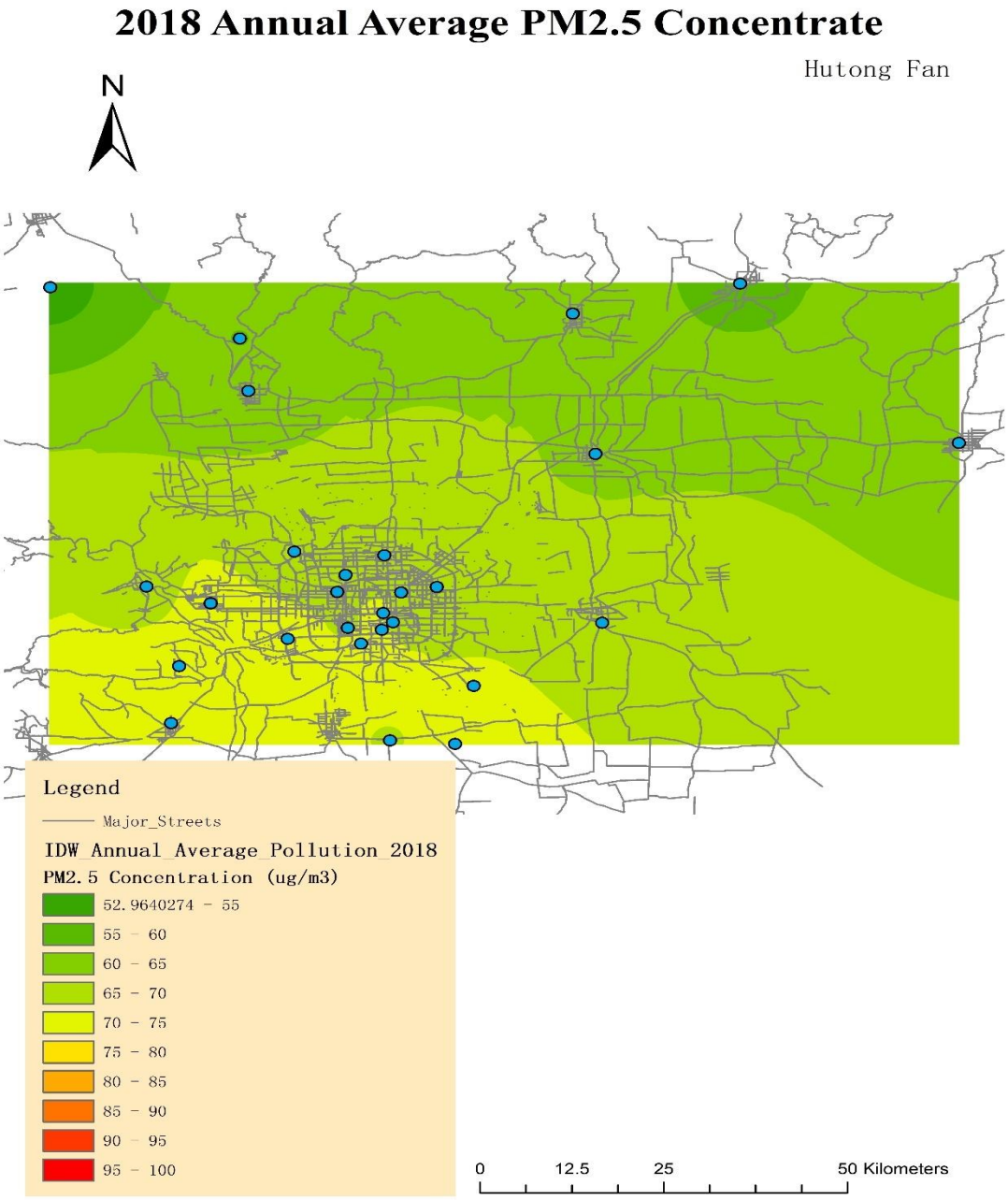

e)

Figure 6: Results of Average Annual Spatial Distribution Patterns (ug/ m³)
a) 2014, b) 2015, c) 2018, d) 2017, e) 2018

Examples of average seasonal distribution patterns of the five daily sampling time periods are shown in Figure 7.Map legends of seasonal distribution patterns based on daily sampling time were also standardized for better visualization and comparisons. In this distribution series of $PM_{2.5}$ air pollution, the highest average $PM_{2.5}$ concentration value rangesfrom 190 to 200 ug/m3, and the lowest average $PM_{2.5}$ concentration value rangesfrom 20 to 30 ug/m3. Comparing the seasonal changes of thefive different daily monitoring time periods, we found that spatial distribution patterns of the $PM_{2.5}$ concentrations also change in different seasons. Distribution patterns of daily sampling time periods during the spring, fall and winter seasons show that the area of least $PM_{2.5}$ pollutions is still in the north and northwest part in Beijing, while the area ofhighest $PM_{2.5}$ pollutions is still in the south and southeast region of Beijing (Figure 7 a)). However, the daily sampled $PM_{2.5}$ air pollution patterns in the summertime are more evenly distributed across the Beijing municipality. In the summer season, the area most affected by $PM_{2.5}$ air pollution is the core urban area or in downtown Beijing, as well as the south and southeast region of Beijing (Figure 7 b).

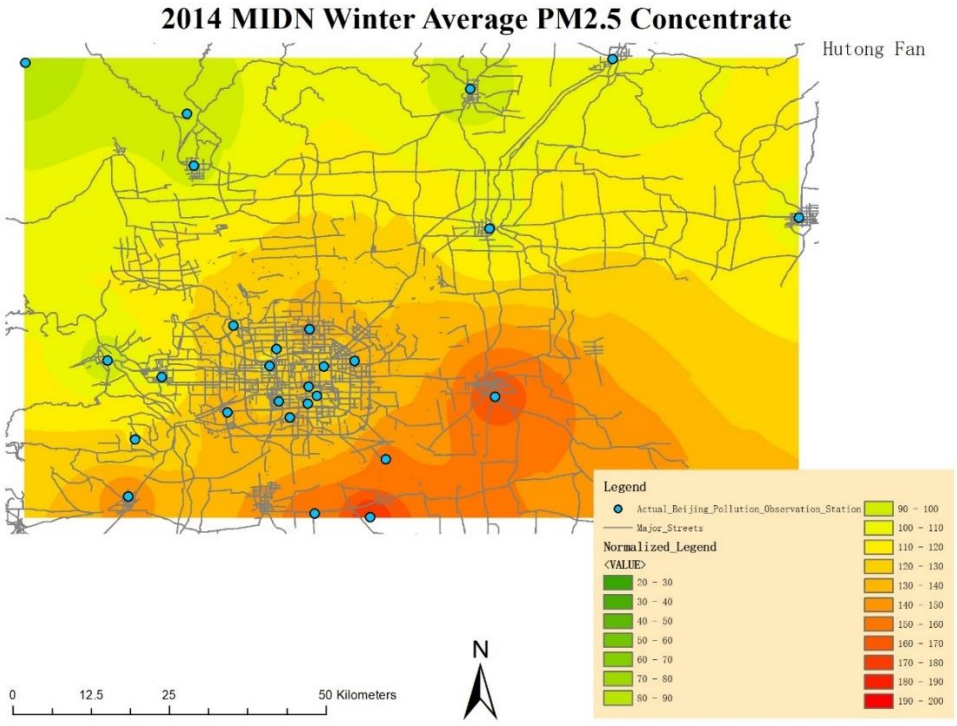

a)

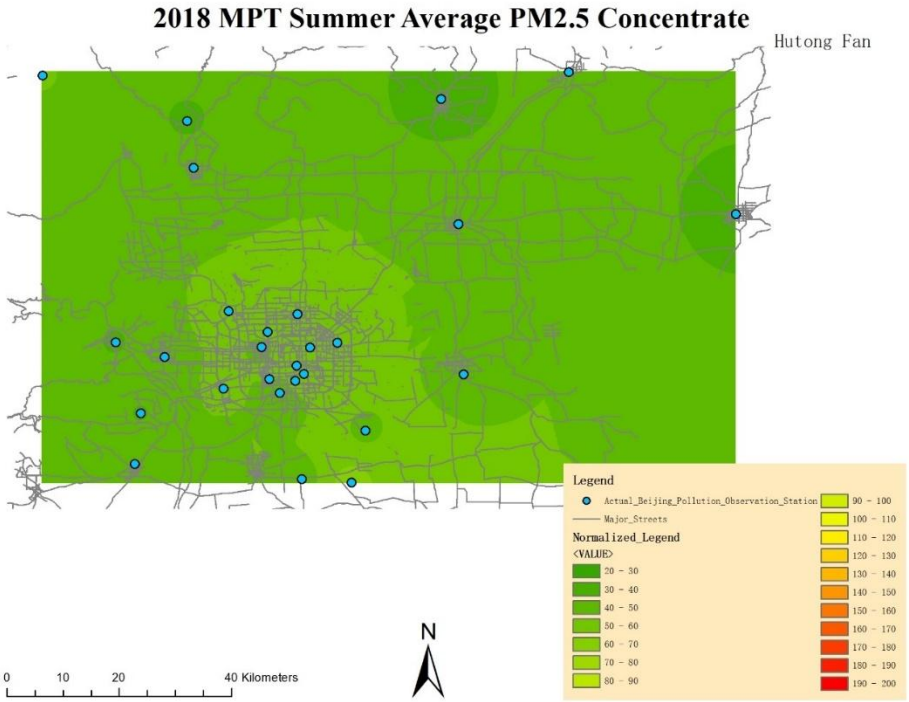

b)

Figure 7: $PM_{2.5}$ Contaminant Spatial Distribution Variation (ug/m³)
a) 2014 MIDN Winter Average $PM_{2.5}$ Concentrate Map, b) 2018 MPT Summer Average $PM_{2.5}$Concentration Map

Sample results of spatial interpolations of five daily surveying time periods by seasons are shown in Figure 8. This research found that heavy $PM_{2.5}$ air pollution often occurred during the wintertime when heat energy suppliesfor commercial, office, and residential buildings were conducted. During winter seasons, midnight periods (MIDN) of the entire five years presented the highest $PM_{2.5}$ air pollution concentrations. This evidence strongly suggests that heating supply to buildings and houses is a major $PM_{2.5}$ air pollution source in our study area. Since the lowest temperature always occurs during midnight (MIDN) period, coal or natural gas combustion for heating supply reaches the highest. The heating supply facilities for buildings and houses need to consume more coals or fuels and increase the combustion to maintain the indoor temperature higher than 16℃according to government guideline (The Government of Beijing Municipality, 2020). This process in turn produced more $PM_{2.5}$ air pollutions.

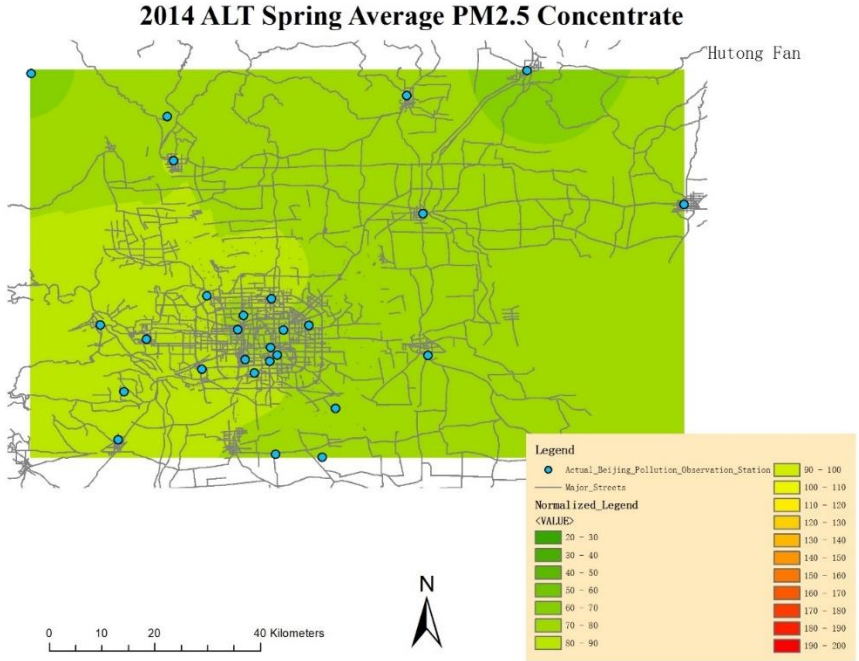
2014 ALT Spring Average PM2.5 Concentrate
Hutong Fan
Legend
Actual_Beijing_Pollution_Observation_Station
Major_Streets
Normalized_Legend
<VALUE>
20 - 30
30 - 40
40 - 50
50 - 60
60 - 70
70 - 80
80 - 90
90 - 100
100 - 110
110 - 120
120 - 130
130 - 140
140 - 150
150 - 160
160 - 170
170 - 180
180 - 190
190 - 200
N
0 10 20 40 Kilometers

a)

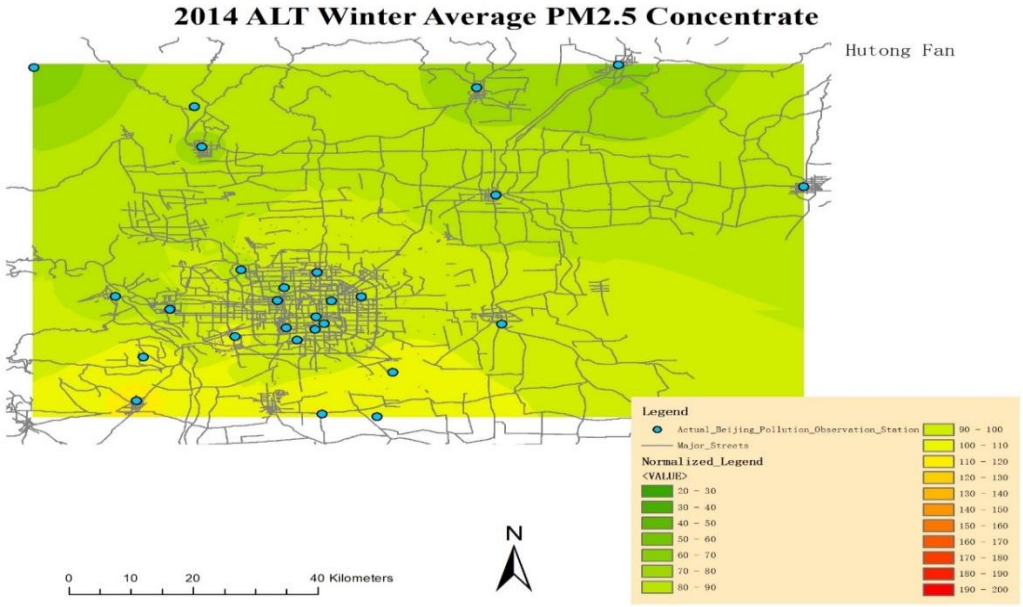
2014 ALT Winter Average PM2.5 Concentrate
Hutong Fan
Legend
Actual_Beijing_Pollution_Observation_Station
Major_Streets
Normalized_Legend
<VALUE>
20 - 30
30 - 40
40 - 50
50 - 60
60 - 70
70 - 80
80 - 90
90 - 100
100 - 110
110 - 120
120 - 130
130 - 140
140 - 150
150 - 160
160 - 170
170 - 180
180 - 190
190 - 200
N
0 10 20 40 Kilometers

b)

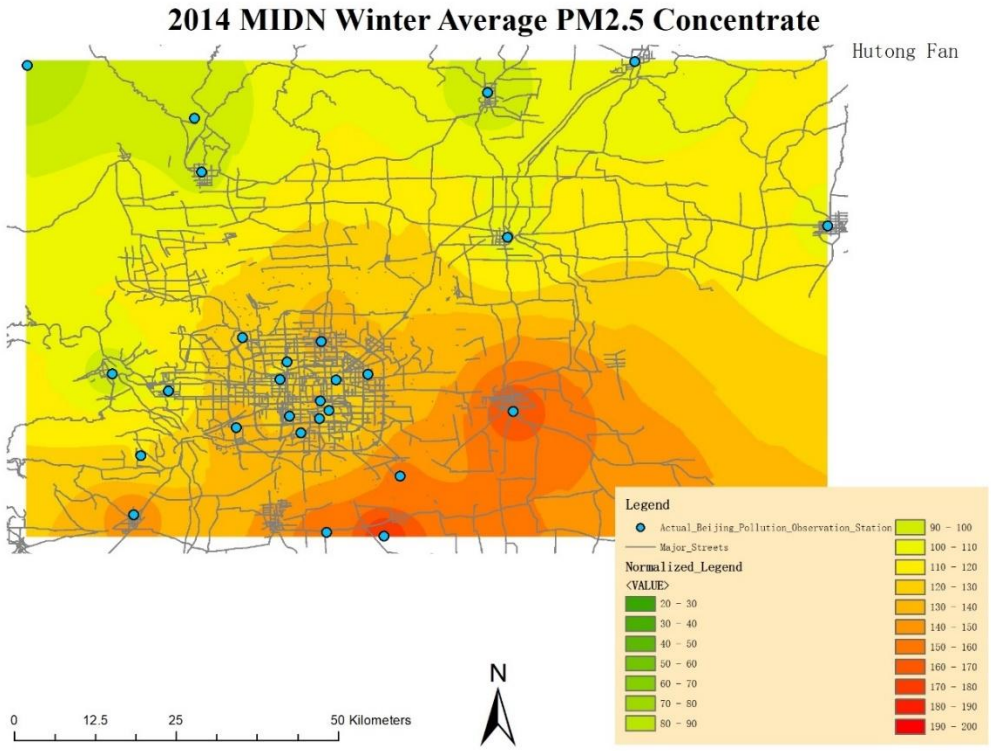
2014 MIDN Winter Average PM2.5 Concentrate
Hutong Fan
Legend
Actual_Beijing_Pollution_Observation_Station
Major_Streets
Normalized_Legend
<VALUE>
20 - 30
30 - 40
40 - 50
50 - 60
60 - 70
70 - 80
80 - 90
90 - 100
100 - 110
110 - 120
120 - 130
130 - 140
140 - 150
150 - 160
160 - 170
170 - 180
180 - 190
190 - 200
N
0
12.5
25
50 Kilometers

c)

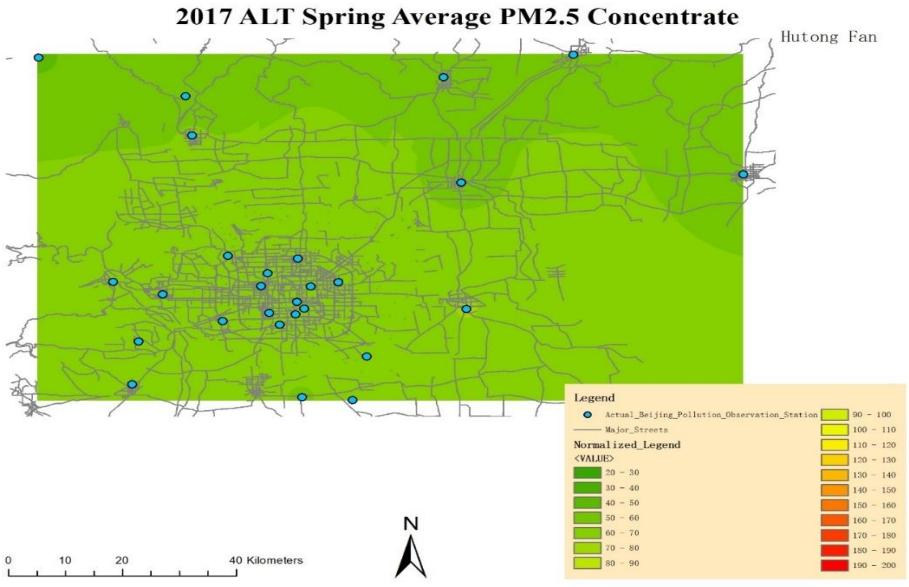
2017 ALT Spring Average PM2.5 Concentrate
Hutong Fan
Legend
Actual_Beijing_Pollution_Observation_Station
Major_Streets
Normalized_Legend
<VALUE>
20 - 30
30 - 40
40 - 50
50 - 60
60 - 70
70 - 80
80 - 90
90 - 100
100 - 110
110 - 120
120 - 130
130 - 140
140 - 150
150 - 160
160 - 170
170 - 180
180 - 190
190 - 200
N
0
10
20
40 Kilometers

d)

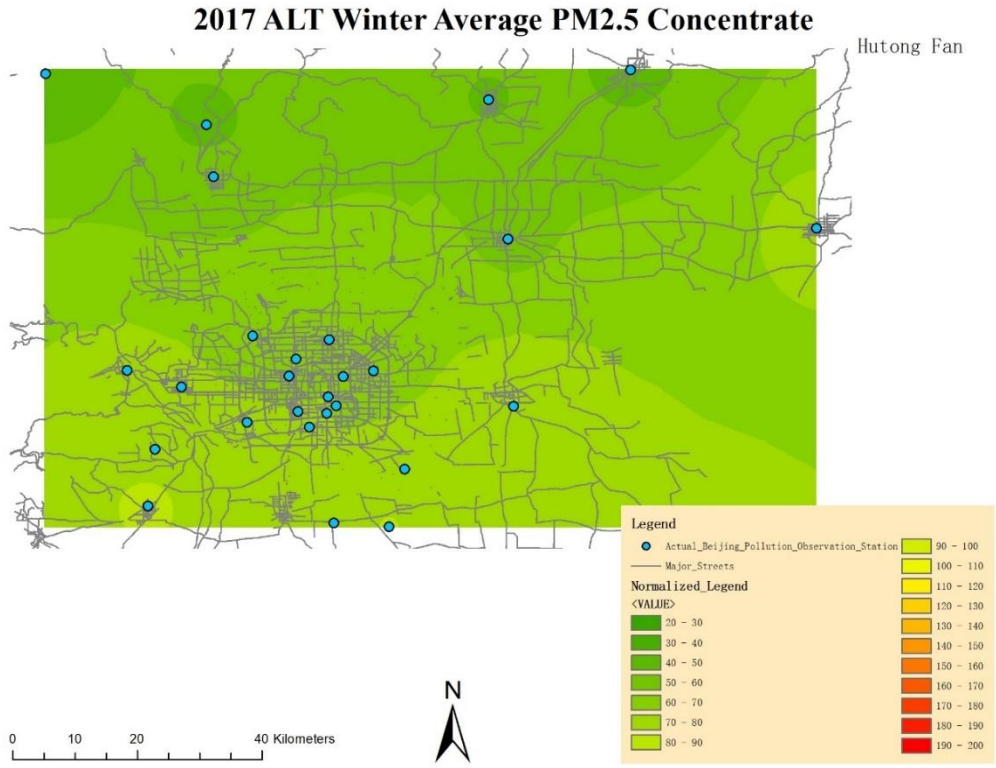

e)

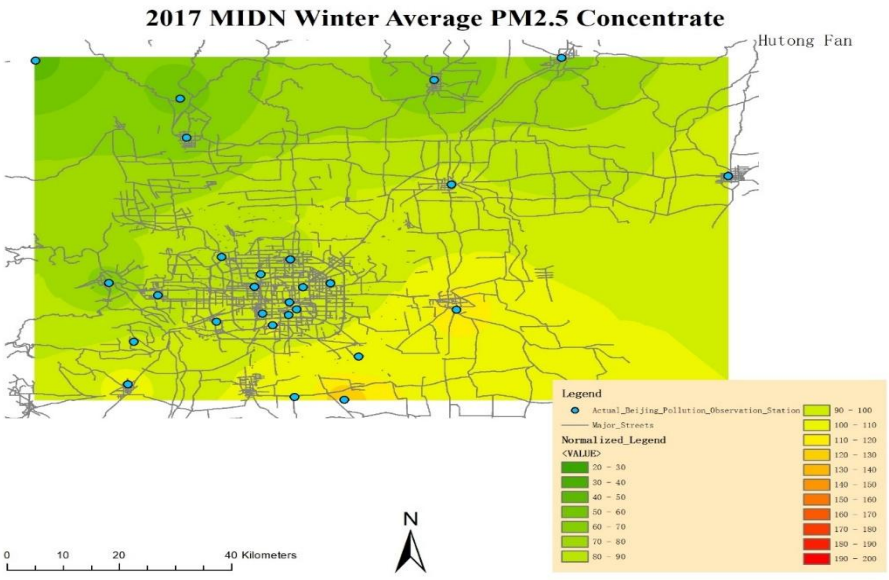

f)

Figure 8: Severe $PM_{2.5}$ Contaminant Situation in Wintertime (ug/m³)

a) 2014 Spring ALT Average $PM_{2.5}$ Concentrate Map, b) 2014 ALT Winter Average $PM_{2.5}$ Concentrate Map, c) 2014 MIDN Winter Average $PM_{2.5}$ Concentrate Map, d) 2017 Spring ALT Average $PM_{2.5}$ Concentrate Map, e) 2017 ALT Winter Average $PM_{2.5}$ Concentrate Map, f) 2017 MIDN Winter Average $PM_{2.5}$ Concentrate Map

This research also found that the $PM_{2.5}$ air pollutions were decreasing during the study period across five daily sampling times and during the different seasons year by year. According to Figure 9, even during the sampling time of most heavy $PM_{2.5}$ air pollutions, the midnight (MIDN) in winter season each year, the $PM_{2.5}$ pollution concentrations show the trendof decline. Assuming the level of heat energy supply to buildings and houses in winter kept the same, the decreasing of $PM_{2.5}$ air pollution concentrations should mainly be credited to the government policy of converting coal combustion to natural gas combustion, to electricity heating, as well as clean coal technology replacement (Xie et al., 2019).

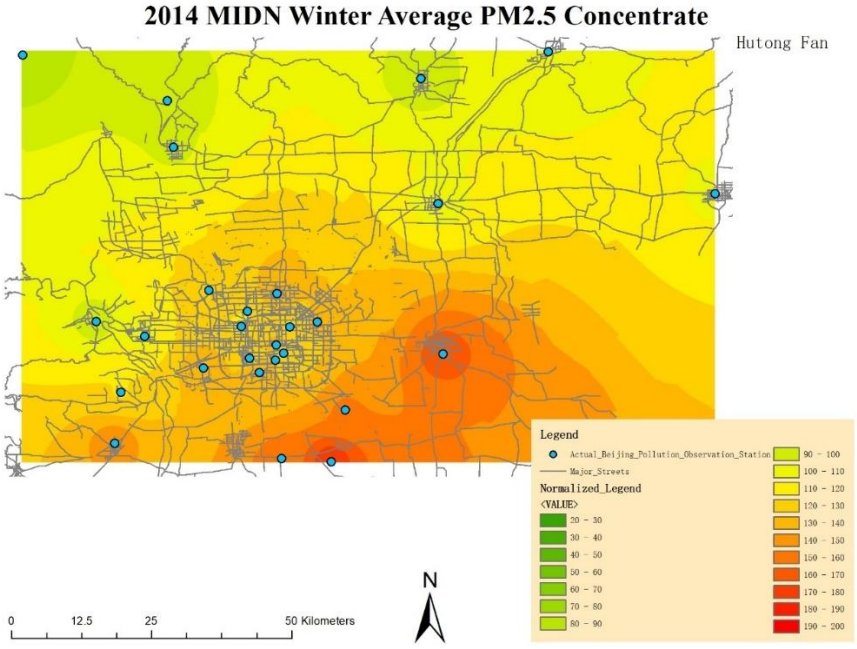

a)

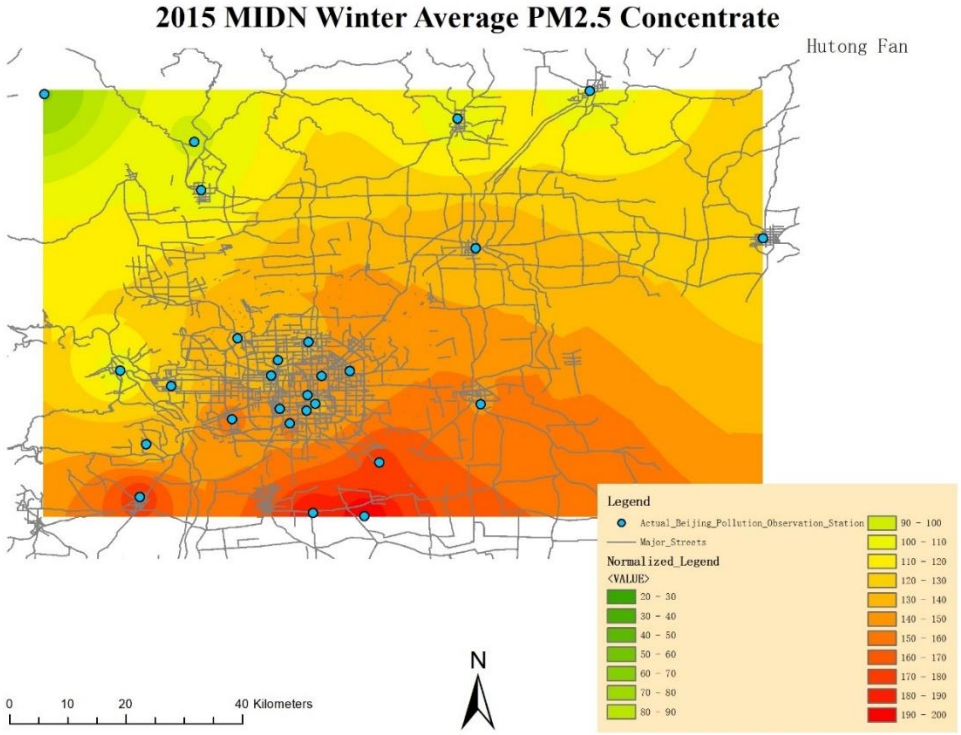
2015 MIDN Winter Average PM2.5 Concentrate
Hutong Fan
Legend
Actual_Beijing_Pollution_Observation_Station
Major_Streets
Normalized_Legend
<VALUE>
20 - 30
30 - 40
40 - 50
50 - 60
60 - 70
70 - 80
80 - 90
90 - 100
100 - 110
110 - 120
120 - 130
130 - 140
140 - 150
150 - 160
160 - 170
170 - 180
180 - 190
190 - 200
N
0 10 20 40 Kilometers

b)

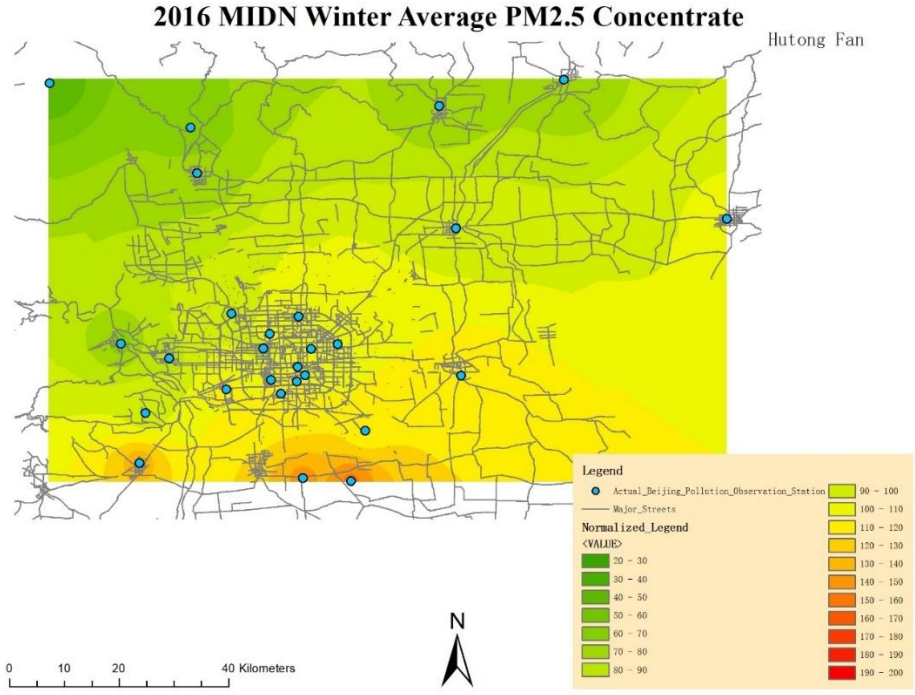
2016 MIDN Winter Average PM2.5 Concentrate
Hutong Fan
Legend
Actual_Beijing_Pollution_Observation_Station
Major_Streets
Normalized_Legend
<VALUE>
20 - 30
30 - 40
40 - 50
50 - 60
60 - 70
70 - 80
80 - 90
90 - 100
100 - 110
110 - 120
120 - 130
130 - 140
140 - 150
150 - 160
160 - 170
170 - 180
180 - 190
190 - 200
N
0 10 20 40 Kilometers

c)

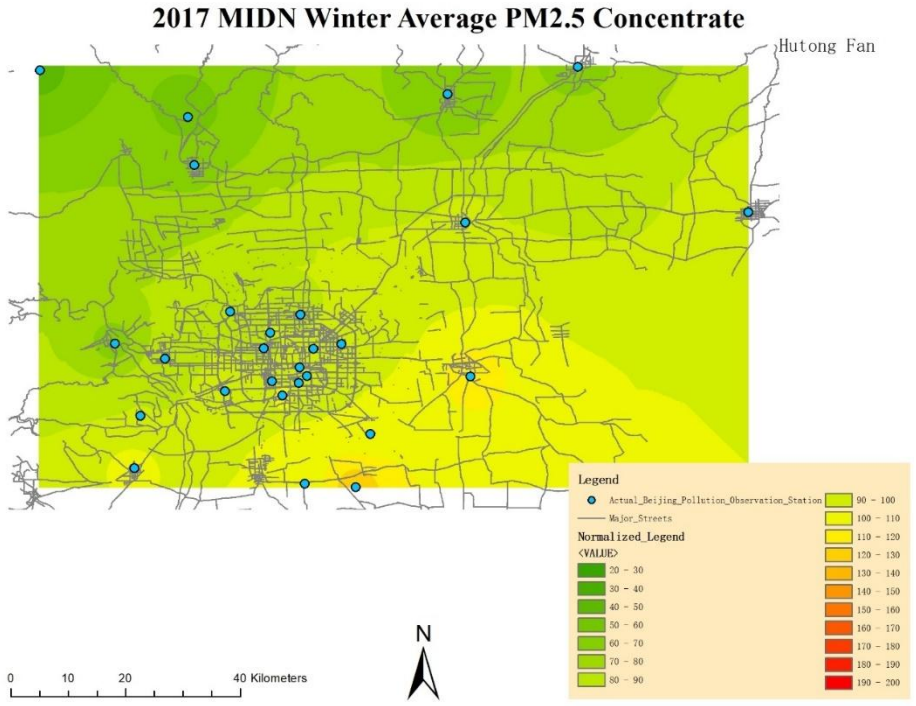
2017 MIDN Winter Average PM2.5 Concentrate
Hutong Fan
Legend
Actual_Beijing_Pollution_Observation_Station
Major_Streets
Normalized_Legend
<VALUE>
20 - 30
30 - 40
40 - 50
50 - 60
60 - 70
70 - 80
80 - 90
90 - 100
100 - 110
110 - 120
120 - 130
130 - 140
140 - 150
150 - 160
160 - 170
170 - 180
180 - 190
190 - 200
N
0 10 20 40 Kilometers

d)

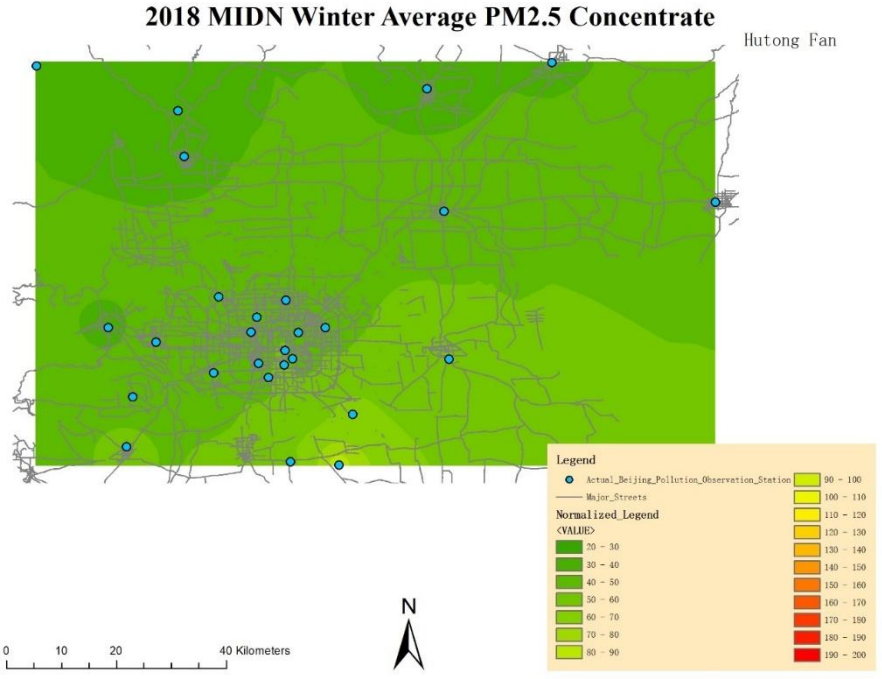
2018 MIDN Winter Average PM2.5 Concentrate
Hutong Fan
Legend
Actual_Beijing_Pollution_Observation_Station
Major_Streets
Normalized_Legend
<VALUE>
20 - 30
30 - 40
40 - 50
50 - 60
60 - 70
70 - 80
80 - 90
90 - 100
100 - 110
110 - 120
120 - 130
130 - 140
140 - 150
150 - 160
160 - 170
170 - 180
180 - 190
190 - 200
N
0 10 20 40 Kilometers

e)

Figure 9: The Decreasing Trend of $PM_{2.5}$ Pollutant within MIDN Winter Sample Time (ug/m³)
a) 2014 MIDN Winter Average $PM_{2.5}$ Concentrate Map, b) 2015 MIDN Winter Average $PM_{2.5}$ Concentrate Map, c) 2016 MIDN Winter Average $PM_{2.5}$ Concentrate Map, d) 2017 MIDN Winter Average $PM_{2.5}$ Concentrate Map, e) 2018 MIDN Winter Average $PM_{2.5}$ Concentrate Map

Figure 10 indicates that the gradients of $PM_{2.5}$ concentration declining in the study area also decrease during the five-year period. Comparing the APT sampling time period in winter with that in the summer in 2018, the gradient is much lower than that during 2014. The decreasing of $PM_{2.5}$ air pollution gradients during the study years and in the study area show the strong reduction of $PM_{2.5}$ pollution and represents the result of government policy in improving the air quality in Beijing.

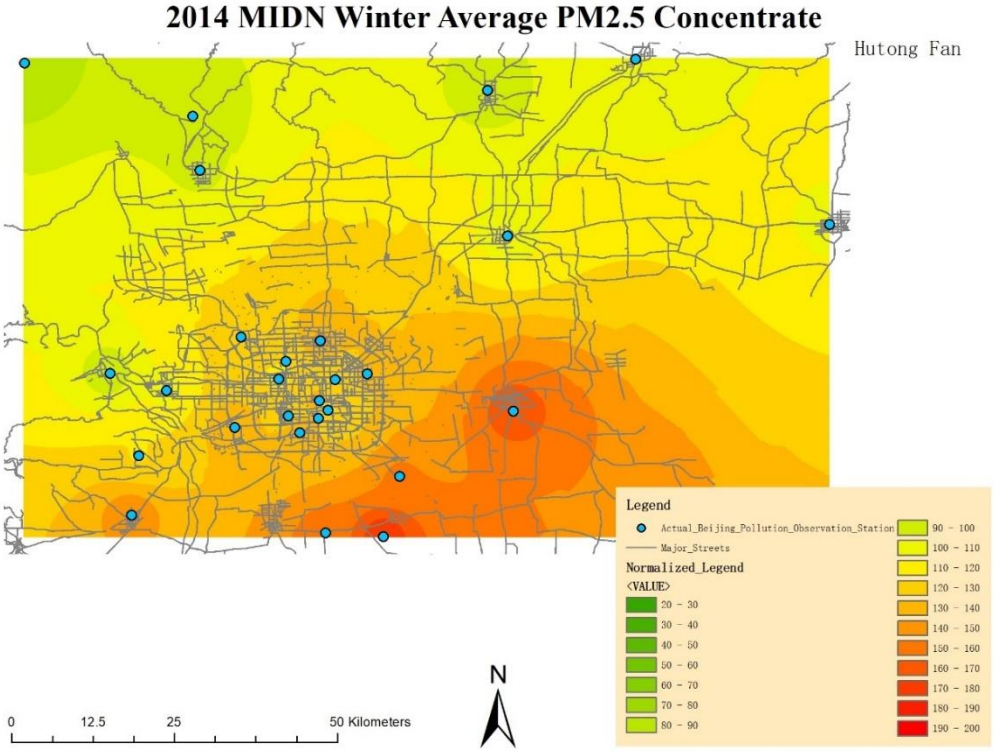

a)

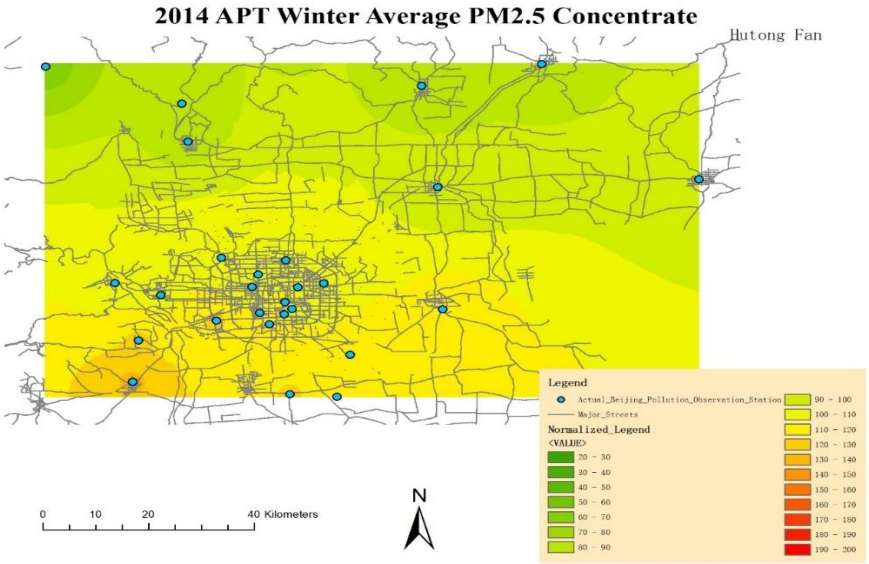
2014 APT Winter Average PM2.5 Concentrate
Hutong Fan
Legend
Actual_Beijing_Pollution_Observation_Station
Major_Streets
Normalized_Legend
<VALUE>
20 - 30
30 - 40
40 - 50
50 - 60
60 - 70
70 - 80
80 - 90
90 - 100
100 - 110
110 - 120
120 - 130
130 - 140
140 - 150
150 - 160
160 - 170
170 - 180
180 - 190
190 - 200
0 10 20 40 Kilometers
N

b)

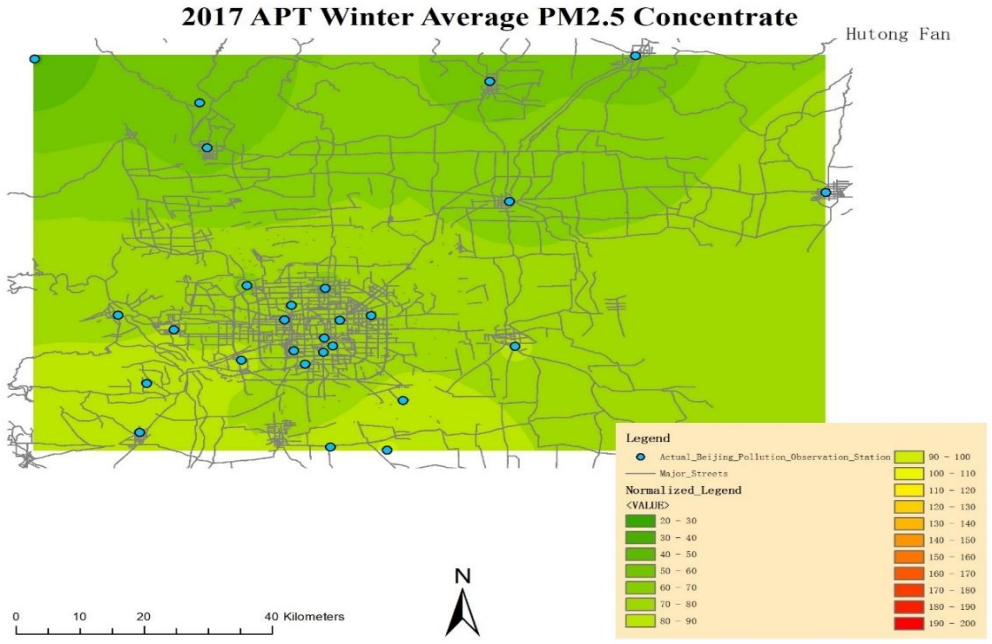
2017 APT Winter Average PM2.5 Concentrate
Hutong Fan
Legend
Actual_Beijing_Pollution_Observation_Station
Major_Streets
Normalized_Legend
<VALUE>
20 - 30
30 - 40
40 - 50
50 - 60
60 - 70
70 - 80
80 - 90
90 - 100
100 - 110
110 - 120
120 - 130
130 - 140
140 - 150
150 - 160
160 - 170
170 - 180
180 - 190
190 - 200
0 10 20 40 Kilometers
N

c)

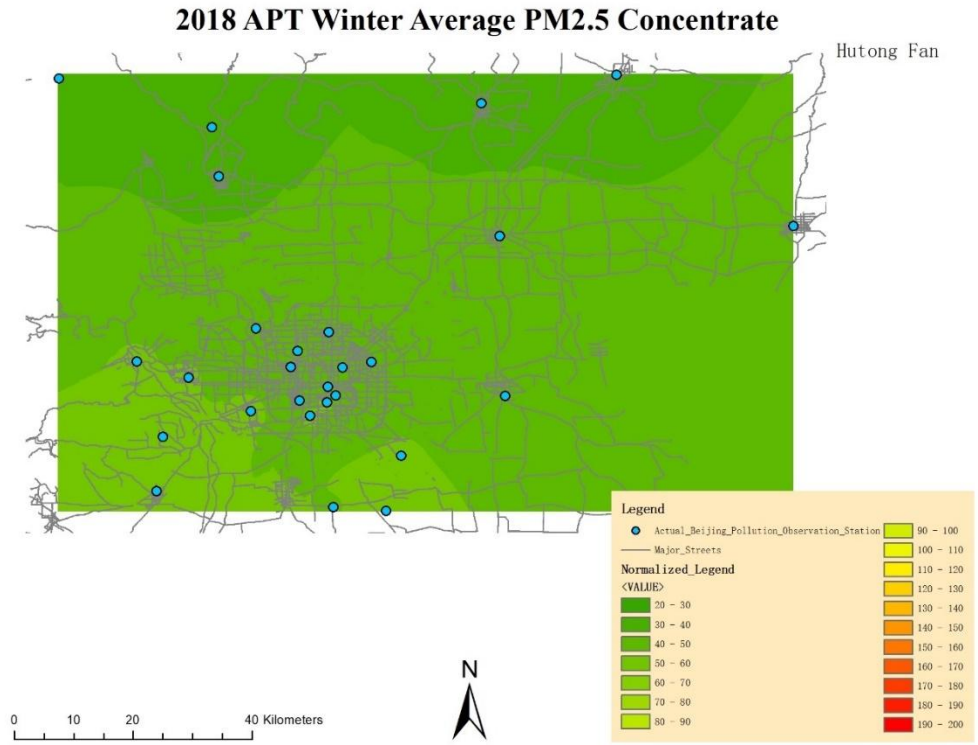

d)

Figure 10: The Descending of $PM_{2.5}$ Contaminant Concentration Gradients (ug/m³)
a) 2014 MIDN Winter Average $PM_{2.5}$ Concentrate Map, b) 2014 APT Winter Average $PM_{2.5}$ Concentrate Map, c) 2017 APT Winter Average $PM_{2.5}$ Concentrate Map, d) 2018 APT Winter Average $PM_{2.5}$ Concentrate Map

In summary, this research discovered the following.First, winter is the most severe period of $PM_{2.5}$ air pollution in each meteorological year. PCA results indicatethat the $PM_{2.5}$ air pollution peaks in each of PCA graph plots during the winter season each year. The results of Seasonal Average Distribution Patterns show that most of the high $PM_{2.5}$ air pollution concentrations occur during the winter season, especially during the midnight (MIDN) sample time periods (Figure 9 and 10).

Secondly, the $PM_{2.5}$ air pollution concentrations in Beijing were gradually decreasing from 2014 to 2018. The evidence to support this conclusion are from PCA results (Figure 5) and Results of Average Annual Spatial Distribution Patterns (Figure 6). The results of PCA show the fluctuation decline of the air pollution from 2014 to 2018 (Figure 5). Standardized Result Atlas of Average Annual Spatial Distribution Patterns (Figure 6) show the improvement of the air quality during the study period.

Thirdly, in terms of a five-year time perspective, Mann-Kendall Trend Analysis shows the reductions of $PM_{2.5}$ air pollutions in summer, autumn, and winter seasons (Table 2, Table 3,and Table4). Although there are a few observation sites (5 of 27) support there are no obvious up or down trends among spring samplings of $PM_{2.5}$ air pollution concentrations during the five-year period

(Table 1), most of observation sites (22 of 27) support that there is descending trend (significant or weak trend) in the spring seasons during the five-year period. The most rigorous emission reduction policy in Chinese history, "Air Pollution Prevention and Control Action Plan" that was enacted by the Chinese government in 2013 and the actions to comply with this policy may cause the overall improvement of air quality and declining trend of $PM_{2.5}$ air pollution in Beijing (Zhao et al., 2018).

Fourthly, the $PM_{2.5}$ air pollution concentrations in summer are significantly lower than that in other seasons. According to the results of PCA analysis (Figure 5), the values of $PM_{2.5}$ air pollution concentration are the lowest during the summer comparing to other seasons. Meanwhile, based on the Result Atlas of Average Seasonal Distribution Patterns (Figure 6), even in the most polluted years, the highest $PM_{2.5}$ pollution concentration range is lower than 80 ~ 90 ug/m3 level (Figure 11) in summers.

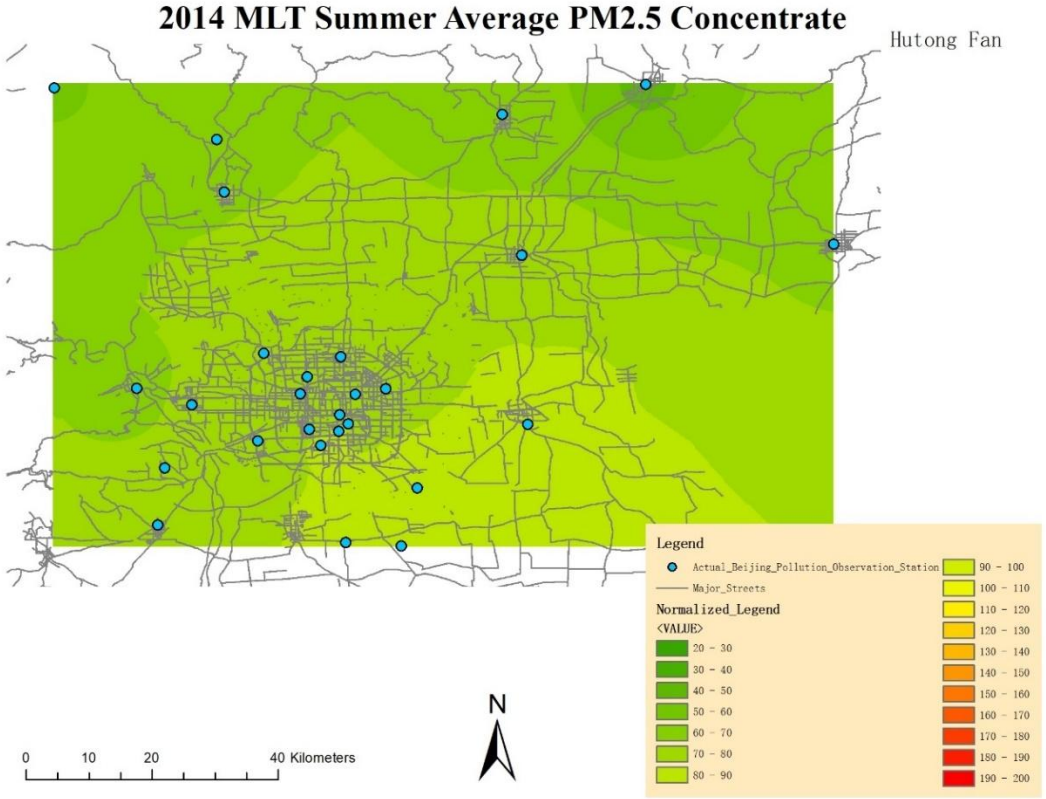

a)

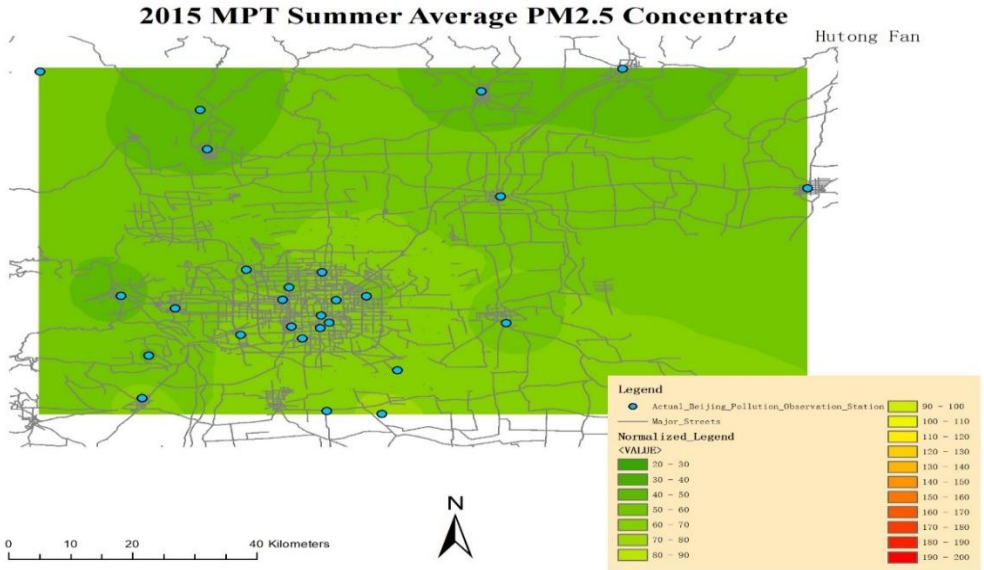

b)

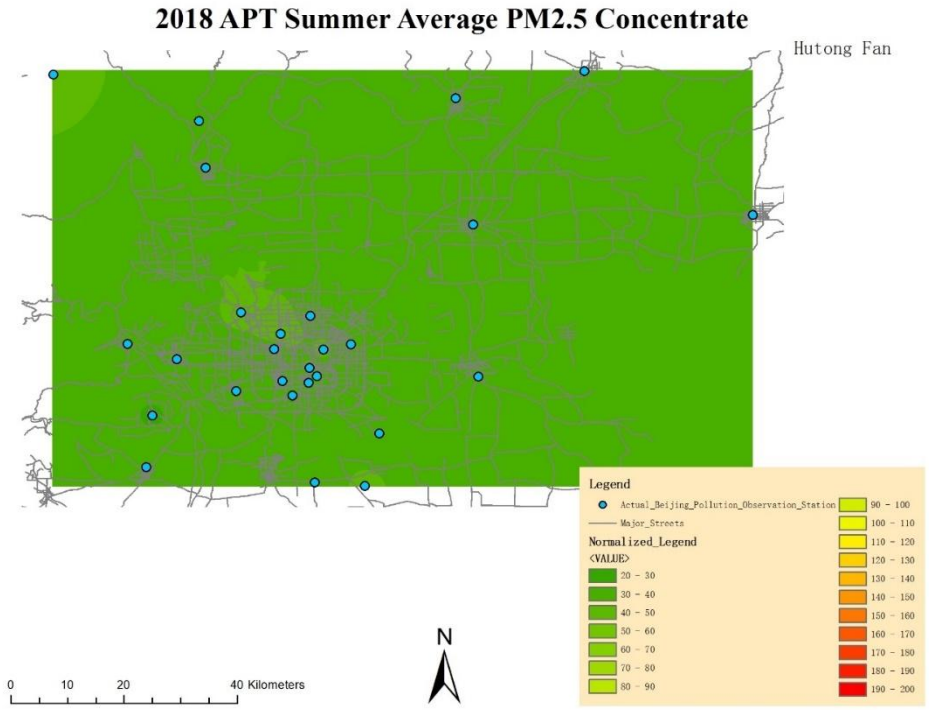

c)

Figure 11: Better $PM_{2.5}$ Contaminant Situation in Summertime (ug/m³)
a) 2014 MLT Summer Average $PM_{2.5}$ Concentrate Map, b) 2015 MPT Summer Average $PM_{2.5}$ Concentrate Map, c) 2018 APT Summer Average $PM_{2.5}$ Concentrate Map

Fifthly, spatial distribution patterns show the area of lowest $PM_{2.5}$ pollutions in Beijing is north and northwest region (Figure 6, 7). The highest concentrations of $PM_{2.5}$ air pollution in the northwest part in Beijing occurred during midnight (MIDN) in 2014 winter (Figure 12). The $PM_{2.5}$ air pollution concentration record at Badaling Observation Site reached to the 80 ~ 90 ug/m3 level. Also, the most polluted area is in the south and southeast part of Beijing. The core urban area in Beijing is not the most polluted regions according to both Annual Average Concentrate Atlas (Figure 6) and Result Atlas of Seasonal Average Distribution Patterns (Figure 7, 8, 9, 10, and 11).

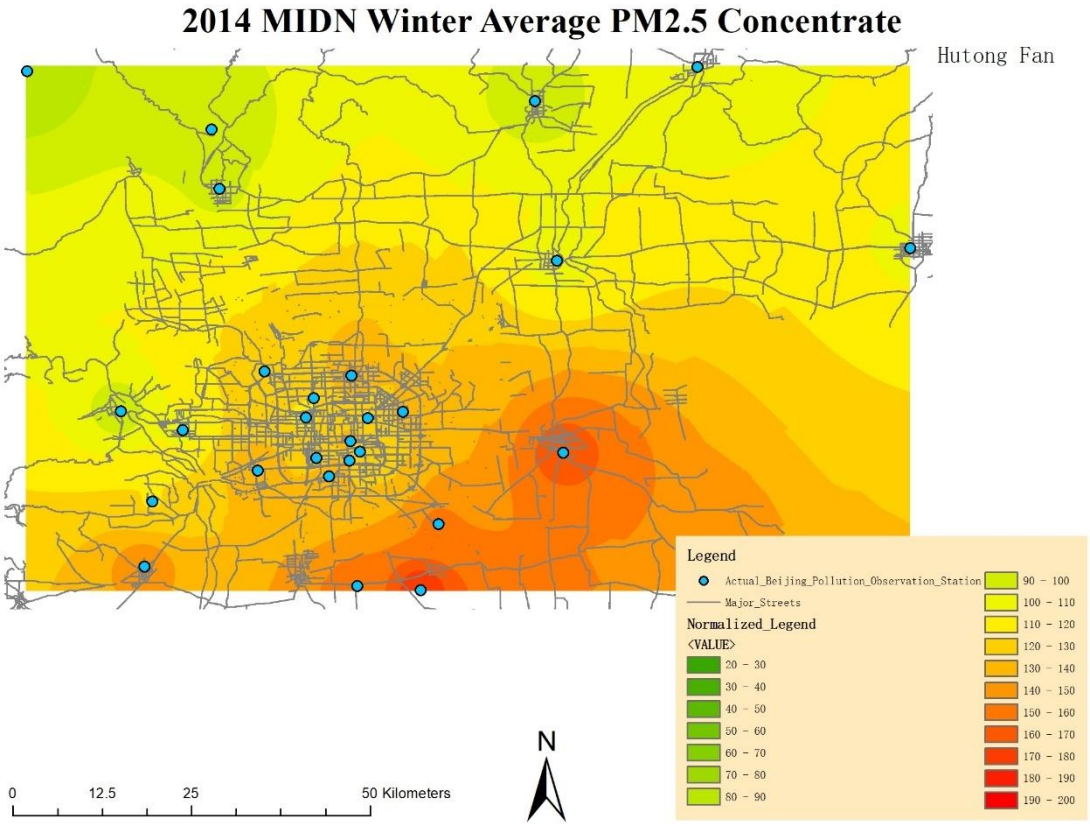

Figure 12: 2014 MIDN Winter Average $PM_{2.5}$ Concentrate Map (ug/m³)

Sixthly, the results of this research suggest that vehicle traffic volume may not be the major influential factor of $PM_{2.5}$ air pollution in Beijing. The Result Atlas of Seasonal Average Distribution Patterns (Figure 13) does not show significant high level of $PM_{2.5}$ air pollution concentrations during the peak traffic time periods, nor does it show high values in the dense road network area in the study region. However, the interpolation patterns might be impacted by the locations and density of air pollution monitoring stations. Further studies are needed.

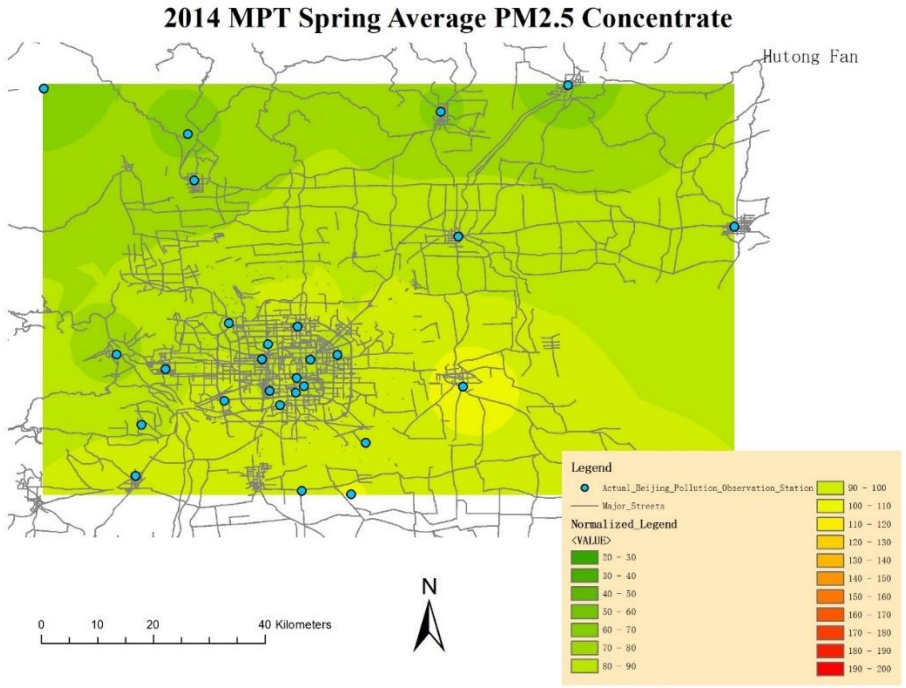
2014 MPT Spring Average PM2.5 Concentrate
Hutong Fan
Legend
Actual_Beijing_Pollution_Observation_Station
Major_Streets
Normalized_Legend
<VALUE>
20 - 30
30 - 40
40 - 50
50 - 60
60 - 70
70 - 80
80 - 90
90 - 100
100 - 110
110 - 120
120 - 130
130 - 140
140 - 150
150 - 160
160 - 170
170 - 180
180 - 190
190 - 200
0 10 20 40 Kilometers
N

a)

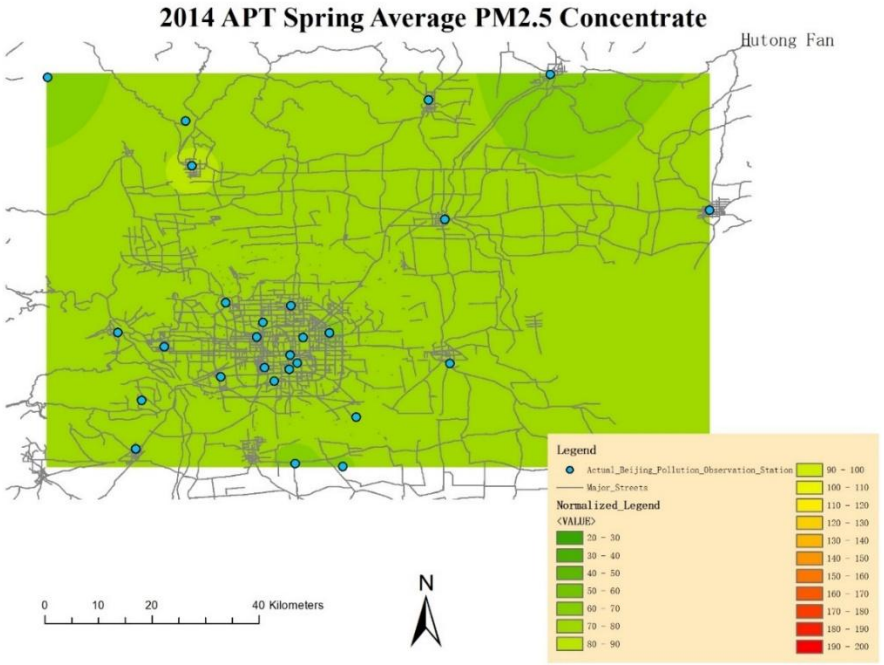
2014 APT Spring Average PM2.5 Concentrate
Hutong Fan
Legend
Actual_Beijing_Pollution_Observation_Station
Major_Streets
Normalized_Legend
<VALUE>
20 - 30
30 - 40
40 - 50
50 - 60
60 - 70
70 - 80
80 - 90
90 - 100
100 - 110
110 - 120
120 - 130
130 - 140
140 - 150
150 - 160
160 - 170
170 - 180
180 - 190
190 - 200
0 10 20 40 Kilometers
N

b)

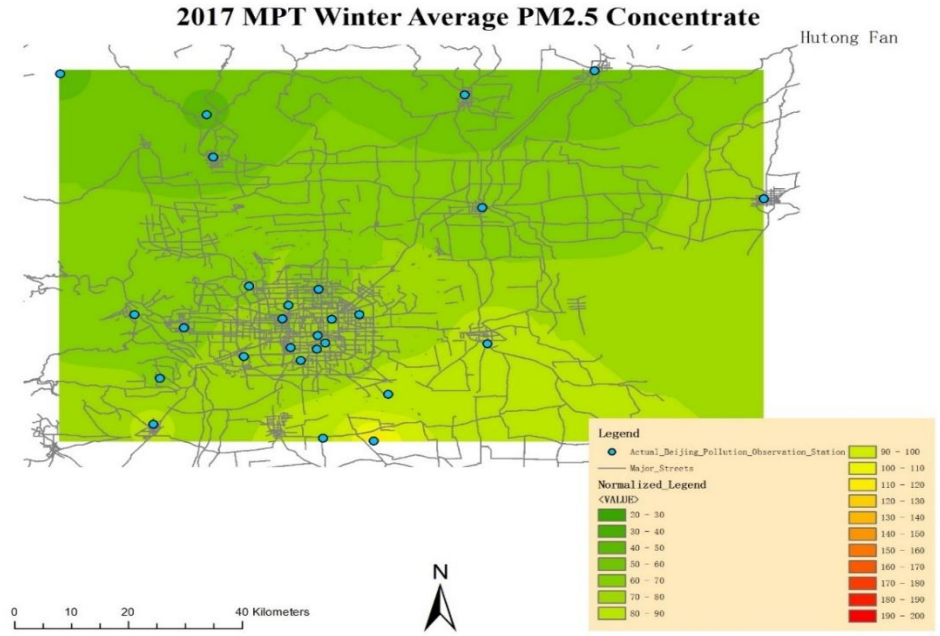

c)

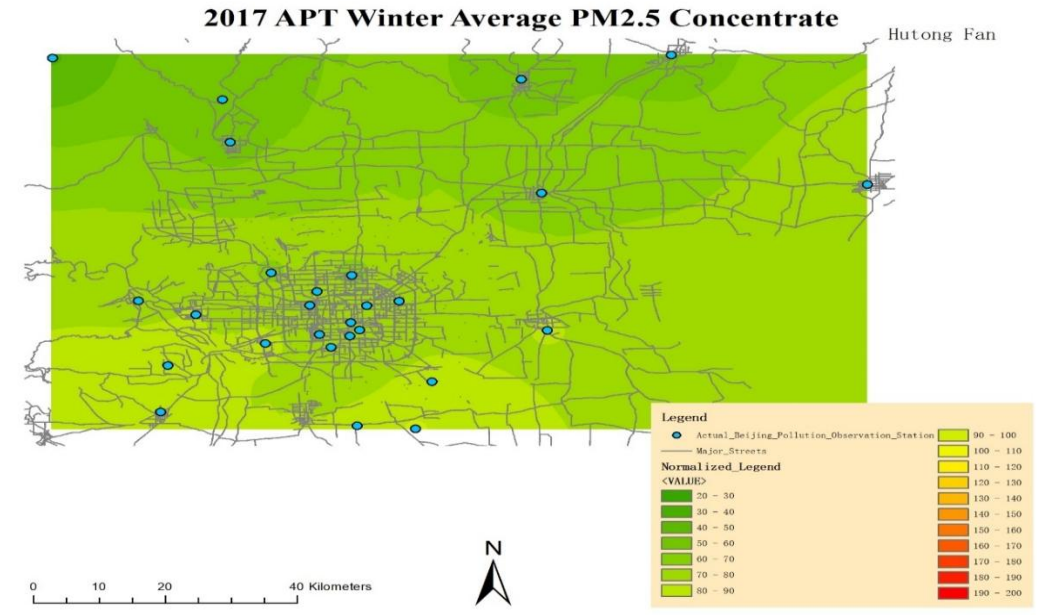

d)

Figure 13: Selected Part of the MPT and APT Sample Time Periods' Map (ug/m³)
a) 2014 MPT Spring Average $PM_{2.5}$ Concentrate Map, b) 2014 APT Spring Average $PM_{2.5}$ Concentrate Map, c) 2017 MPT Winter Average $PM_{2.5}$ Concentrate Map, d) 2017 APT Winter Average $PM_{2.5}$ Concentrate Map

Seventhly, winter season heat energy supply to buildings and houses generated great impacts to the $PM_{2.5}$ air pollution concentrations in Beijing. According to the Result Atlas of Average Distribution Patterns (Figure 7 and 8), the $PM_{2.5}$ concentrations in winter are the highest in each meteorological year. The selection of time period of winter season in this research coincides with that of building and house heating supply in Beijing (The Government of Beijing Municipality, 2020). The analytical results of this research indicate building and house heating in winter contributed a great amount of $PM_{2.5}$ air pollution during the season. It makes the winter season as the highest air pollution season. While, implementing the rigorous emission reduction policy "Air Pollution Prevention and Control Action Plan" enacted in 2013 (Zhao et al., 2020), the $PM_{2.5}$ pollution was gradually reduced in the winter. Figure 9 clearly indicates the improvement of air quality and reduction of $PM_{2.5}$ pollution in winter seasons, in particular for midnight (MIDN) time periods. Owing to the policy actions of converting coal combustion to electricity or natural gas, or clean coal technology replacement (Xie et al., 2019), the proportion of fossil fuel consumptions in heating supply activities gradually declined year by year. According to the Winter Heating Clean Energy Planin Northern China (2017-2021) (Chinese Central Government Policy Group on Finance and Economics, 2016), the percentage of clean energy heating supply in the northern region in China should reach 50% by the end of 2019, and 74 million tons of CO2 should be reduced from the coal consumptions and from discontinuations of inefficient small furnaces. As the result of multiple government policies and macro-management, the pollution from winter heat supply decreased during this research time (2014 ~ 2018).

5. Conclusion

This research analyzed temporal and spatial patterns using a five-year hourly monitored large $PM_{2.5}$ air pollution dataset. The focus of this research is the data processing and analysis for the big $PM_{2.5}$ air pollution dataset itself. In the future, we can combine the population distribution data to analyze the impacts to the $PM_{2.5}$ pollutions by population density. We can also combine the temperature variations and weather condition data to gain better understanding to the winter heating supply factor on $PM_{2.5}$ air pollutions. According to research of Li (2016), the distribution of $PM_{2.5}$ in Beijing area is obviously affected by the surrounding regions. The process of $PM_{2.5}$ pollutant dispersion was greatly influenced by the landscape and weather conditions in Beijing. Therefore, exploring the dispersion process of $PM_{2.5}$ pollutants with the terrain around Beijing using a big dataset will also be significant in the future studies. In addition, we can also improve the accuracy of our spatial pattern analysis. For example, the standardized legend of Average Distribution Patterns could have higher contrast ratio and more precise $PM_{2.5}$ pollution concentration categories.

References

Beck, H. E., Zimmermann, N. E., McVicar, T. R., Vergopolan, N., Berg, A., & Wood, E. F. (2020). Publisher Correction: Present and future Köppen-Geiger climate classification maps at 1-km resolution. Scientific Data, 7(1), 1-2.

Cao, J.B., Chi, D.C., Wu, L.Q., Liu, L., Li, S.Y., Yu, M. (2008). Study on the application of Mann-kendall test method in the analysis of precipitation trends. Agricultural Technology and Equipment. 4 :(5).

Central Government of China, Commission on Finance and Economic Development. (2016). Northern Region Winter Clean Heating Plan (2017-2021), 678pp (online).

Chen, C., Wen, J.J., Wang, B.Y., Fang, J.H., Lang, J.D., Tian, G., Jiang, J.K., Zhu, T.F. (2014) Inhalable Microorganisms in Beijing's PM2.5 and PM10 Pollutants during a Severe Smog Event. Environmental Science & Technology, 48(3), 1499-1507. DOI: 10.1021/es4048472.

Deligiorgi, D. and Philippopoulos, K. (2011). Spatial Interpolation Methodologies in Urban Air Pollution Modeling: Application for the Greater Area of Metropolitan Athens, Greece, Advanced Air Pollution, Dr. Farhad Nejadkoorki (Ed.), InTech, DOI: 10.5772/17734.

Fan, S.B., Tian, L.D., Zhang, D.X., Qu, S. (2015) Emission Characteristics of Vehicle Exhaust in Beijing Based on Actual Traffic Flow Information. Environmental Science, 36(8): 2750-2757.

Gimond, M. (2021). Intro to GIS and Spatial Analysis. Retrieved November 29, 2021, from https://mgimond.github.io/Spatial/index.html

Joshua, S.A., Michael, B., Aaron J.C., Majid E., C, Arden, P. (2018). Ambient PM2.5 Reduces Global and Regional Life Expectancy. Environmental Science & Technology Letters, 5(9), 546-551.

Karmeshu, N. (2012). Trend Detection in Annual Temperature & Precipitation using the Mann Kendall Test – A Case Study to Assess Climate Change on Select States in the Northeastern United States.

Li, L. (2016). The Spatial Distribution Patterns of $PM_{2.5}$ as Observed before, During and after APEC Period in Beijing. 2016 24TH INTERNATIONAL CONFERENCE ON GEOINFORMATICS (GEOINFORMATICS).

Lozano, A., Usero, J., Vanderlinden, E., Raez, J., Contreras, J., Navarrete, B., Bakouri, H.E. (2009). Design of air quality monitoring networks and its application to 2 and O3 in Cordova, Spain. Microchemical Journal, 93 No. 2, (November 2009), 211 219, 0002-6265X.

Meng, T., Wang, J.M., Yan, H.F. (2006). Web evolution and incremental crawling. Journal of Software, 17(5):1051−1067. http://www.jos.org.cn/1000-9825/17/1051.htm

Ministry of Ecology and Environment of the People's Republic of China. (2013). Technical Specifications for Installation and Acceptance of Ambient Air Quality Continuous Automated Monitoring System for PM10 and PM2.5 (HJ 655-2013)

Shlens, J. (2014). A tutorial on principal component analysis. arXiv preprint arXiv:1404.1100.

Tang, T., W. H. Zhao, W. Zhao, H. Gong, and L. Cai, (2009). GIS analysis of spatial and temporal changes of air particulate concentrations and their impacts on respiratory diseases in Beijing, China. Middle States Geographe, Volume 42, 73-82

Tang T., W. Zhao, H. Gong, X. Li, K. Zang, W. H. Zhao, Bernosky J. D., and S. Li, (2010). GIS spatial analysis of population exposure to fine particulate air pollution in Beijing, China. Environmental GeoSciences. Vol. 17 No. 01: 1-16

The People's Government of Beijing Municipality. (2020, June 29). Beijing Heating Tips. The People's Government of Beijing Municipality. Retrieved from http://english.beijing.gov.cn/livinginbeijing/housing/202005/t20200513_1895777.html.

Wu, X., Zhu, B., Zhou, J., Bi, Y., Xu, S., & Zhou, B. (2021). The epidemiological trends in the burden of lung cancer attributable to PM2.5 exposure in China. BMC Public Health, 21(1), 1-8.

Xie L.Y., Chang Y.X., Lan Y. (2019). *The Effectiveness and Cost-Benefit Analysis of Clean Heating Program in Beijing*. Chinese Journal of Environmental Management, 11(3): 87-93.

Zhao Mingzhu, Wang Dan, Fang Jie, Li Yan, & Mao Jun. (2020). Metro station temperature prediction based on LSTM neural network. Journal of Beijing Jiaotong University, 44(04), 94.

Zhao Mingzhu, Wang Dan, Fang Jie, Li Yan, & Mao Jun. (2020). Metro station temperature prediction based on LSTM neural network. Journal of Beijing Jiaotong University, 44(04), 94.

Zheng, G.J., Duan, F.K., Su, H., Ma, Y.L., Cheng,Y., Zheng, B., Zhang, Q., Huang, T., Kimoto, T., Chang, D., Pöschl, U., Cheng, Y.F., He, K.B. (2015). Exploring the severe winter haze in Beijing: the impact of synoptic weather, regional transport and heterogeneous reactions. Atmos. Chem. Phys. 15, 2969-2983. https://doi.org/10.5194/acp-15-2969-2015.